Università
Ca'Foscari
Venezia

Master's degree programme
in Biotechnologies for Sustainable
Development and the Environment

Final Thesis

Phototrophic purple bacteria (PPB) biomass production from wine lees

Supervisor
Ch. Prof. Francesco Valentino

Graduand
Giada D'Ambrosio
Matriculation Number 897576

Academic Year
2023 / 2024

Index

1. Introduction 1

1.1. Winery wastes 2

1.1.1. Wine lees (WL) 3

1.2. Purple phototrophic bacteria (PPB) 6

1.2.1. Metabolism 6

1.2.2. Biorefinery approach 8

1.3. Aquaculture 11

1.3.1. PPB value in aquaculture 12

2. Thesis objective.....16

3. Materials and methods 17

3.1. Mixed microbial culture PPB..... 17

3.2. Feedstock preparation..... 19

3.3. Experimental configuration and cycle schedule 19

3.4. Samples preparation..... 21

3.5. Recirculation of the biomass 22

3.6. Carbohydrate, lipid and protein characterization..... 22

3.7. Analytical methods 23

3.7.1. SCFAs and ethanol..... 23

3.7.2. Total solids and volatile solids 23

3.7.3. Soluble chemical oxygen demand (sCOD) 24

3.7.4. Ammonium analysis..... 25

3.7.5. PHA analysis 25

3.7.6. Carbohydrates, lipids and proteins content 27

3.8. Calculations 28

4. Results and discussion 30

4.1 Photobioreactor operation: Run–1 30

4.1.1 Feedstock characterisation 30

4.1.2 Photobioreactor performances 32

4.2 Photobioreactor operation: Run–2 38

4.2.1 Feedstock characterisation 38

4.2.2 Photobioreactor performances 40

4.2.3 Biomass nutritional profile characterisation 45

4.3 Photobioreactor operation: Run-3 45

4.3.1 Feedstock characterisation 45

4.3.2 Photobioreactor performances 48

4.3.3 Biomass nutritional profile characterisation 52

4.4 Comparison between SBR runs 53

5. Conclusions 56

References 58

1. Introduction

Wine industry is one of the most economically significant sectors in the food industry, with estimated world wine production at 258 millions of hectolitres (Mhl) in 2022. According to the International Organisation of Vine and Wine (OIV), Italy is one of the major vine-growing countries, with 718’000 hectares of vineyard area (OIV, 2022). Italy (49.8 Mhl), France (45.6 Mhl), and Spain (35.7 Mhl) are the leading wine-producing countries. Moreover, Italy has emerged as the largest exporter in 2022 with 21.9 mhl, accounting for 20% of the global exports. The increasing number of wineries generates significant quantities of organic waste and their uncontrolled breakdown can affect the environment in multiple ways, such as the release of greenhouse gases into the atmosphere (Ahmad et al., 2020), phytotoxic effects on plants (Moldes et al., 2008) and various adverse effects on soils, including nitrogen immobilization and increased soil electrical conductivity (Paradelo et al., 2013). Therefore, effective and sustainable waste management is crucial to mitigate these negative environmental impacts (Ahmad et al., 2020). Traditionally, companies have prioritized paying fines over investing in sustainable waste management solutions, despite the existence of the “polluter pays” principle, due to the historically low level of sanctions imposed on polluting companies. However, the growing environmental concerns have driven authorities to seek solutions for recycling and valorizing waste products, leading to significantly increased fines (Devesa-Rey et al., 2011). Thus, the “polluter pays” principle is becoming less profitable, and companies must explore new strategies for valorizing their by-products (De Iseppi et al., 2020). As stated in ISO 14000, there is an urgent need for industries to reduce their environmental impacts (Oliveira & Duarte, 2016). Finally, recent European and national policies on circular bioeconomy promote the use of food by-products and waste, including those generated by wine production, as secondary raw materials for the transition from a linear to a circular economy, thereby increasing the sustainability of the food supply chain (Gottardo et al., 2022).

1.1. Winery wastes

The winemaking process for white and red wines is shown in Figure 1.

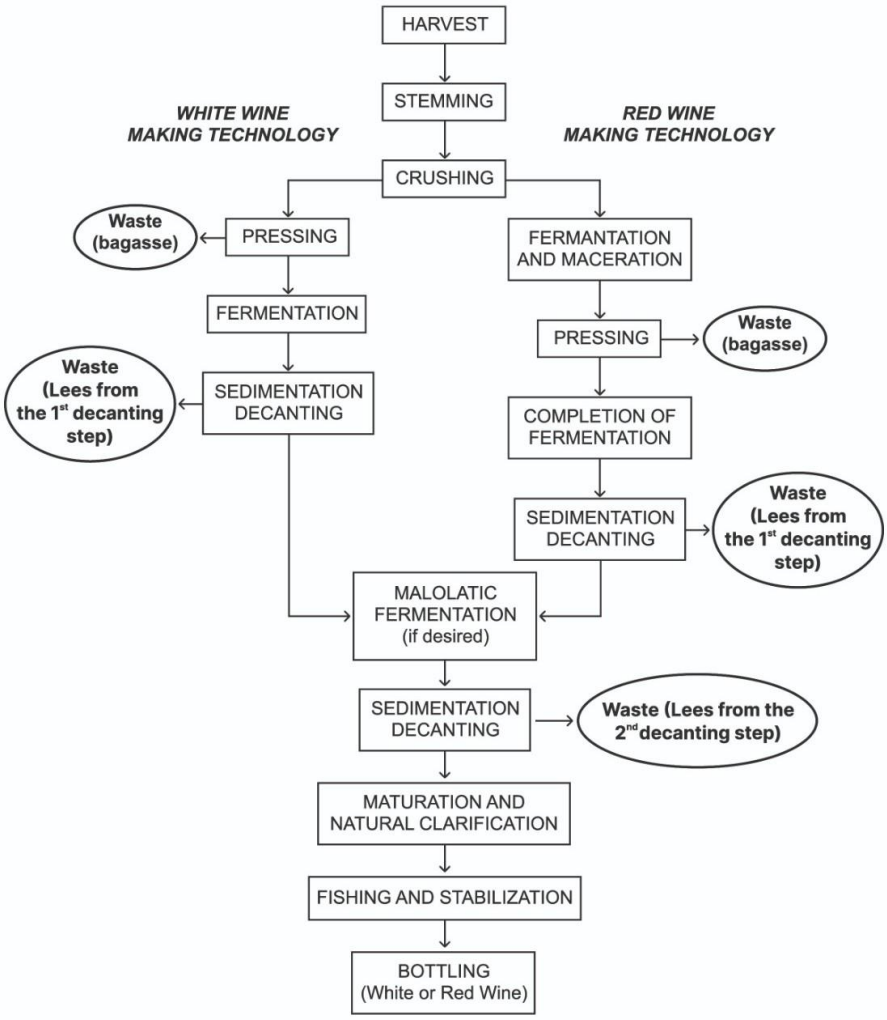

Figure 1: Scheme of vinification process for white and red wine production (Moldes et al., 2008).

Wine industry generates different residues characterized by high contents of biodegradable compounds and suspended solids (Navarro et al., 2005). As a result of this process, one ton of grapes approximately generates 0.13 tons of grape marc, 1.65 m^3 of wastewater, 0.03 tons of stalks and 0.06 tons of lees. No significant differences were observed for grape marc, lees and wastewater ratios across different years or wineries (Oliveira & Duarte, 2016). Grape marc, the solid residue generated during winemaking, is composed of fibrous components such as skin, seeds, and stems (Ahmad et al., 2020). Grape skin, a significant component of grape marc, represents a valuable source of polyphenols and triterpenes, which can be extracted for nutraceuticals, pharmaceuticals and cosmetics applications (Ruberto et al., 2007).

Indeed, several studies have highlighted the high antioxidant and polyphenol content of grape marc, making it a promising natural source of these compounds (Rockenbach et al., 2011). Seeds and stems are rich in lignin and cellulose, two components that can be valorized respectively to obtain phenols and as a substrate for anaerobic fermentation (Ahmad et al., 2020). Winery wastewater (WW) derives from multiple operations in wine production, including stemming, crushing of grapes, fermentation of the liquid phase, solid-liquid separation following fermentation, clarification and stabilization of the produced wine (Bolzonella et al., 2019). WW primarily contains ethanol, glucose, fructose, and tartaric acid, while red wine WW is particularly rich in polyphenols, including p-coumaric, cinnamic, caffeic, gentisic, ferulic, tannic, and vanillic acids (Gottardo et al., 2022). WW is primarily used for biogas production via anaerobic digestion, offering at the same time a potential for volatile fatty acid (VFA) production, with limited research in scientific literature focused on its acidogenic fermentation (Gottardo et al., 2022). In addition, the presence of ethanol and glucose in WW makes it a suitable substrate for caproic acid production through chain elongation (Kucek et al., 2016).

1.1.1. Wine lees (WL)

According to the European Council Regulation No. 79/337, wine lees is defined as ‘‘the muddy residue accumulating in wine vessels after fermentation or during the storage of wine, dried or not” (EEC Regulation No.337/79). During the alcoholic fermentation of the must, yeasts undergo rapid multiplication, consuming sugars and other nutrients. As these nutrients become depleted, and the environment is no longer conducive to their growth, the yeast cells cease their metabolic activity and ultimately die. The dead yeast cells, along with other microorganisms, suspended solids, colloids, and organic matter, settle at the bottom of the barrels, forming lees (Devesa-Rey et al., 2011). Moreover, wine lees can be obtained as a residue following filtration or centrifugation process (Ahmad et al., 2020). Wine lees composition is influenced by numerous parameters, mainly related to the yeast strain, grape variety, and winemaking method, resulting in a wide range compositional variations, as evidenced by data reported in the literature (De Iseppi et al., 2020). Furthermore, white wine and red wine lees composition can differ significantly, further influenced by the type of wine and the number of decanting steps performed. White wine lees, particularly non-distilled lees,

are generally richer in carbon and nitrogen content (C= $\frac{10.9\ g}{100\ g\ dry\ basis}$, N= $\frac{0.7\ g}{100\ g\ dry\ basis}$, compared to the value after distillation (C= $\frac{6.4\ g}{100\ g\ dry\ basis}$, N= $\frac{0.4\ g}{100\ g\ dry\ basis}$) (Pérez-Bibbins et al., 2015). Conversely, red wine lees behaviour is opposite, with the higher contents quantified after distillation (C= $\frac{11.7\ g}{100\ g\ dry\ basis}$; N= $\frac{1.2\ g}{100\ g\ dry\ basis}$) (Pérez-Bibbins et al., 2015). Moreover, red wine lees has higher concentration of metals (Cu, Mg, Fe, Mn, Ca, Al and Zn) in comparison with white wine lees, due to the contact of the fermenting must with the grape skins (Bustos et al., 2004). Total solids, ashes, nitrogen and carbon contents are generally higher in the first decanting step in white or red wine lees because they have higher concentration of dead yeast and solids in suspension, such as other microorganisms and organic matter, than in the second one (Pérez-Bibbins et al., 2015). Eventually, Da Ros et al., (2017) found that the COD in wine lees is mainly present in its soluble form, and the nitrogen and phosphorus levels are limiting factors for bacterial growth compared with the COD concentration. In fact, the COD:N:P ratio in their study was 502:5:1, which is consistent with values reported by Paradelo et al., (2013). In order to provide a specific example of liquid wine lees composition, in their study Pérez-Bibbins et al., (2015) analyzed the composition of the wine lees (WL) employed in the experiment, as detailed in Table 1.

Table 1: Wine lees liquid fraction characterization, adapted from (Pérez-Bibbins et al., 2015)

pH	3.5 ± 0.23
N (%)	0.62 ± 0.037
C (%)	5.2 ± 0.054
C/N ratio	8.5 ± 0.44
Lactic acid (g/L)	0.4
Citric acid (g/L)	1.3
Malic acid (g/L)	3.6
Tartaric acid (g/L)	3.6
Glycerol (g/L)	5.7
Acetic acid (g/L)	0.5
Ethanol (g/L)	83.7
Phenolic compounds (mg/L)	308.1 ± 0.008
Total N (mg/L)	1,670.8 ± 0.07
Protein (g/L)	n.d

In this study, the liquid fraction of lees contained negligible fermentable sugars, as these are metabolized into ethanol, organic acids during alcoholic fermentation (Pérez-Bibbins et al., 2015). The organic acid profile of lees is influenced by the chemical composition of the raw fruit and subsequent microbial activity. In particular, tartaric, malic, and citric acids are primarily derived from grapes, while lactic acid is produced through malolactic fermentation. Acetic acid, an undesirable byproduct of the oxidation of ethanol by acetic acid bacteria, is typically present in low concentrations (Pérez-Bibbins et al., 2015). Moldes et al., 2008 tested the use of wine lees as soil fertilizers, studying their effect on different plant seeds. Although they were rich in essential nutrients for plants, such as P, K and Mg, the low pH and the high C/N ratio did not lead to seed germination. It has been demonstrated that the concentration of acetic acid and ethanol present in wine lees are high enough to produce phytotoxic effects, making raw wine lees incompatible with direct agricultural application (Moldes et al., 2008). The elevated protein and total nitrogen content, coupled with the significant presence of essential amino acids such as tyrosine, valine and aminocaproic acid, has led to the idea of utilizing wine lees as feed for ruminants (Molina-Alcaide et al., 2008). However, the high amount of polyphenols associated with proteins make a large part of that fraction not assimilable by animals (Devesa-Rey et al., 2011). While the vitamin content of lees is negligible in terms of human nutrition, it provides sufficient levels to support microbial growth (Devesa-Rey et al., 2011). Due to its high organic content, wine lees has been identified as cost-effective nutrient source for the microbial production of various products. Indeed, studies in literature demonstrated that untreated vinification lees may be used either independently or in conjunction with corn steep liquor to formulate cheap and affordable fermentative media to produce lactic acid or xylitol (Bustos et al., 2004). Moreover, recent studies have demonstrated that wine lees can also be processed in an integrated biorefinery. Dimou et al., (2015) developed a biorefinery using wine lees as a raw material to produce antioxidants, tartrate, ethanol, and the remaining nutrient rich-stream was then utilized as a fermentation nutrient supplement for polyhydroxybutyrate (PHB) production by *Cupriavidus necator DSM 7237*. Indeed, the valorization of by-products of winemaking to produce PHA has been gaining attention, as it could provide a cheap raw material that would lower the overall cost of PHA production (Gottardo et al., 2022). However, given the recent valorization of these by-products, PHA production has been limited to pure culture systems, whereas mixed microbial culture (MMC) approach still needs to

be implemented (Gottardo et al., 2022). Overall, while wine lees are produced in large quantities worldwide, their commercial exploitation is still limited, and despite their previously discussed potential they are often considered a waste to manage, rather than a valuable resource (De Iseppi et al., 2020).

1.2. Purple phototrophic bacteria (PPB)

Purple phototrophic bacteria (PPB) are a ubiquitous group of anoxygenic phototrophs that are widely distributed throughout the phylogenetic tree of bacteria with many subdivisions, particularly within the Proteobacteria (Capson-Tojo et al., 2020). PPB are composed of purple sulfur bacteria (PSB) and purple non-sulfur bacteria (PNSB) (Neil Hunter et al., 2009). PSB are predominantly photoautotrophic and sulfur-requiring, since reduced sulfur compounds are used as electron donor to reduce inorganic carbon. Additionally, they are able to store S_0 intracellularly and they have limited photoheterotrophic and dark metabolic capabilities (Neil Hunter et al., 2009). In contrast, PNSB exhibit a wider metabolic versatility, capable of photoheterotrophy, photoautotrophy and aerobic or anaerobic chemotrophic growth (Neil Hunter et al., 2009). *Rhodobacter sphaeroides* and *Rhodopseudomonas palustris* are PNSB representatives, serving as model organisms to investigate bio-photo energy generation and carbon and nitrogen fixation (Capson-Tojo et al., 2020; Geyer & Helms, 2006). PPB adsorb light in the near-infrared (NIR) wavelengths, between 805 nm and 1035 nm, via bacteriochlorophyll (BChl) a and b (Capson-Tojo et al., 2020). In addition, an arsenal of more than 75 potential carotenoids, which composition is species dependent, extend the exploitable wavelength range to bands in the ultraviolet (UV) and visible (VIS) light spectra, as well as providing photoprotection (Hartigan et al., 2002).

1.2.1. Metabolism

The diverse range of potential PPB applications arises from the exploitation of their metabolic versatility, simplified in Figure 2 (Capson-Tojo et al., 2020).

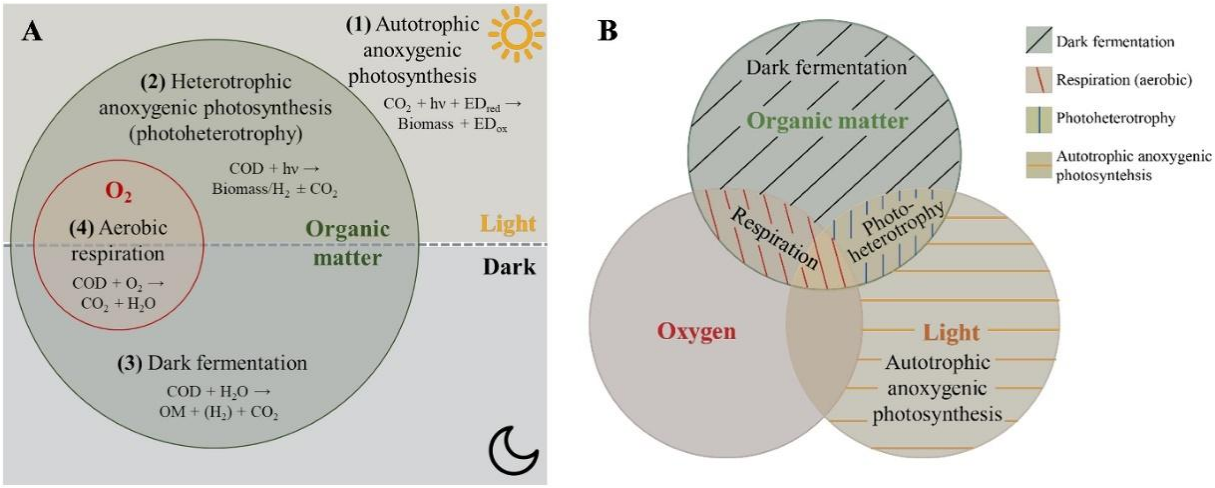

Figure 2: Simplified representations of the main metabolic modes of PPB, (A) structured according to energy and carbon sources and electron acceptors and (B) including the dominant mode under the presence/absence of organic matter, oxygen or light. ED stands for electron donor and COD for chemical oxygen demand (Capson-Tojo et al., 2020)

PPB are capable to grow under anaerobic conditions via three distinct metabolic strategies: photoautotrophy, photoheterotrophy, and fermentation. Photoautotrophic growth involves the utilization of light as energy source, carbon dioxide as carbon source, and a diverse series of inorganic electron donors, such as H_2, H_2S, S_0, $S_2O_3^2$, Fe^{2+}, and NO_2^- (Capson-Tojo et al., 2020). Photoheterotrophic growth also utilizes light as energy source; however, in this case, organic carbon can acts as carbon source and as electron donors, especially acetate, propionate, butyrate and other volatile fatty acids (VFA) (Lu et al., 2019). During fermentation, organic compounds are used as both energy and carbon sources, with glucose, sucrose, lactose and ethanol used as electron donors (Neil Hunter et al., 2009). Moreover, PPB are capable of aerobic growth through respiration and possess the ability to fix dinitrogen gas via nitrogenase enzyme complex (Kim et al., 1999). Environmental conditions, such as type of electron acceptor and donor, and the presence or absence of light or oxygen, have a strong impact on the predominant metabolic growth mode (Capson-Tojo et al., 2020). When light is present and oxygen is absent, anoxygenic phototrophic growth dominates. Under this condition, the primary source of energy is light, which is absorbed by bacteriochlorophylls (BChls) and carotenoids, the pigments required for light harvesting and photosynthetic growth. When neither oxygen nor light are present, fermentation will prevail (Capson-Tojo et al., 2020). When oxygen is present at high concentrations, the aerobic metabolism will dominate regardless of the availability of light, due to the suppression of BChl and carotenoid synthesis under aerobic condition (Yue et al., 2015). It is known that mixed metabolic pathways, such as photo-

fermentation, are possible, and that the combination of chemical catabolism and light energy results in an enhanced overall yield (Capson-Tojo et al., 2020). Focusing on carbon and resource recovery, anaerobic phototrophic energy generation via photophosphorylation has several advantages compared to chemoheterotrophic growth (Capson-Tojo et al., 2020). These include no aeration requirements, the selection and enrichment of PPB in non-sterile environments, thanks to the exclusive capability of adsorbing NIR wavelengths (Hülsen et al., 2022), and biomass yields up to 1.0 $gCOD_{biomass}/gCOD_{removed}$, which leads to higher resource recovery efficiency (Capson-Tojo et al., 2020). In addition, thanks to the cyclic electron transport in anoxygenic photosynthesis, PPB can grow without requiring a dedicated electron donor or acceptor (Capson-Tojo et al., 2020). When a substrate, such as butyric or valeric acid, is more reduced than the biomass, the substrate will serve as both carbon source and electron donor, to enable CO_2 fixation or other electron dissipation pathways, like hydrogen production or the storage of PHA or polyphosphate (Capson-Tojo et al., 2020). In turn, CO_2 will be produced when the substrate is more oxidized than biomass, as in the case of succinic acid and malic acid (Ahmad et al., 2020).

1.2.2. Biorefinery approach

The biorefinery concept emerged as a response to global energy crises and climate change issues caused by industrialization (Ahmad et al., 2020). A biorefinery is an integrated, efficient and flexible strategy that provides a great alternative to environmental problems by converting waste biomass into energy and high-value bio-based products through different processes (Ragauskas et al., 2006; Bilal et al., 2017). Recent literature, including studies on the treatment of industrial and domestic wastewater (Lu et al., 2019) and other urban and agricultural waste effluents (Allegue et al., 2020;Basak et al., 2014), highlights the unique metabolic versatility of PPB for recovering resources. Utilizing waste streams as feedstock, it is possible to obtain several valuable products from PPB cells, such as 5-aminolevulinic acid (5-ALA), single-cell protein (SCP), pigments, hydrogen and polyhydroxyalkanoates (PHA) (Capson-Tojo et al., 2020). PNSB, in particular *Rhodopseudomonas palustris*, has gained attention thanks to its ability to produce extracellularly 5-ALA, a high-value compound that is beneficial for plant growth and often used in agriculture as herbicide, insecticide and growth enhancer (Sakarika et al., 2020). PPB cells can be used as

single cell protein (SCP) thanks to their high protein content and essential amino acid profiles suitable for nutrition, including elevated contents of methionine and cysteine (Capson-Tojo et al., 2020), which are generally low in other options, such as microalgae (Bleakley & Hayes, 2017). It has been also demonstrated that PPB-enriched cultures grown in non-axenic mode have significantly higher or equal protein contents compared to axenic, pure cultures (Capson-Tojo et al., 2020). In addition, recent studies have shown that aminoacids profiles from PPB-enriched cultures are comparable to those of common commercial protein source, such as eggs, soybean or commercial fishmeal (Delamare-Debouteville et al., 2019). Despite the availability of different commercial SCP products, such as UniPortein®, Quorn®, Solein®, SylPro®, Chlorella, and Spirulina for animal feed and human supplements or food ingredients, PPB-based products have yet to enter the consumer market (Capson-Tojo et al., 2020), even though that possibility had already been discussed in 1977 (Shipman et al., 1977). PPB possess an arsenal of carotenoids and bacteriochlorophylls (BChls), which are part of their light harvesting complexes (Neil Hunter et al., 2009). Carotenoids are organic pigments, which commercial production is increasing significantly in various sectors, including food supplements, as well as the chemical, cosmetic and medical industries. Moreover, carotenoids are used as supplements in aquaculture feeds for their antioxidant and disease-preventing properties, and colouring capacity (Capson-Tojo et al., 2020). Carotenoid content in PPB vary between 0.5 and 13 $mg/g_{dry\ biomass}$, and it has been shown that pure culture cultivation using domestic wastewater as carbon source can produce a carotenoid yield comparable to that obtained using malate as carbon source (Capson-Tojo et al., 2020). PPB, similar to any other organism, cannot grow effectively in media deficient in nutrients such as nitrogen, phosphorus, potassium, sulfur and so on. In fact, if the carbon source is present and nutrients are limiting, an excess of reducing power occurs, leading to the formation of hydrogen or to the storage of PHA to maintain redox homeostasis (Capson-Tojo et al., 2020). Hydrogen production by PPB is generally referred to as photofermentation (PF), although the name can be misleading as it is an anaerobic oxidation rather than a fermentation process (Capson-Tojo et al., 2020). Among the organic compounds that PPB can utilize as carbon and electron sources for hydrogen production, substrates such as acetic acid, butyric acid and simple alcohols have been the most widely tested (Capson-Tojo et al., 2020). However, hydrogen yield is influenced by multiple factors, including the amount of organic carbon

stored as PHA, the competing electron demand of the Calvin cycle, and the presence of ammonium, rather than solely by the carbon oxidation state of the substrate (Vasiliadou et al., 2020). Indeed, PF occurs due to nitrogenase activity, which is stimulated when soluble nitrogen sources are limited (Capson-Tojo et al., 2020). As a result, utilizing nitrogen-limited waste streams as feed for hydrogen production via PF represents an attractive option to reduce substrate costs compared to artificial media (Capson-Tojo et al., 2020). In particular, PPB have been widely assessed for hydrogen production from industrial wastewater treatment or streams coming from biorefineries, as well as different agricultural residues (Capson-Tojo et al., 2020). PPB are also able to store PHAs, a class of microbial polyesters that accumulate within microorganisms. These biopolymers exhibit properties similar to synthetic polymers, such as polypropylene, but unlike them they are biodegradable, biocompatible and non-toxic (Muhammadi et al., 2015). The accumulation of PHAs is a natural phenomenon that occurs under nutrient imbalance conditions. Indeed, when carbon is in excess and other essential nutrients, such as nitrogen, phosphorus, or oxygen, are depleted, PHAs serve as intracellular energy and carbon sources, enhancing microbial survival (Anderson & Dawes, 1990). PHA granules can exist in two physical states: an amorphous, intracellular state within living cells and a partially crystalline state after extraction (Laranja & Bossier, 2020). Among all types of PHAs, poly (3-hydroxybutyrate) (PHB), a linear polyester of D(-)-3-hydroxybutyric acid, is the most widely studied and the first discovered (Lemoigne, 1923; Laranja & Bossier, 2020). PPB are able to produce PHB and PHBV (3-hydroxy-butyrate-co-3-hydroxyvalerate), with overall PHA content ranging between 0.04 and 0.62 $g/g_{dry\ biomass}$ (Capson-Tojo et al., 2020). Furthermore, PPB biomass growth and PHA accumulation can be controlled by simply modifying the nutrient availability, without the need for feast famine selection, as when mixed heterotrophic cultures are used (Capson-Tojo et al., 2020). Once again, this is possible thanks to the great PPB metabolism. Specifically, PPB can replenish reduced cofactors, like NADH or NADPH, via PHA synthesis, using ATP generated via photophosphorylation (Fradinho et al., 2016). This allows PPB cultures to accumulate PHA in a permanent carbon feast regime, simplifying the process when compared to the 3 stage feast-famine operation used for mixed culture aerobic PHA accumulation (Fradinho et al., 2016). The final consideration when producing PHA using PPB is the possible loss of electrons to hydrogen production, as previously discussed. In COD-rich and nitrogen limited streams, both hydrogen and PHA synthesis occur

simultaneously (Chen et al., 2012). While hydrogen production can be suppressed by high ammonia levels, PHA accumulation is less sensitive to nitrogen availability. Indeed, if other essential nutrients, such as phosphorus, magnesium, or sulfur, are limiting, PHA synthesis will proceed even in the presence of high ammonia concentrations (Melnicki et al., 2009).

1.3. Aquaculture

For the first time in history, aquatic animals production from aquaculture exceeded that of capture fisheries in 2022: of the 185 million tonnes of aquatic animals produced, 51% (94 million tonnes) derived from aquaculture and 49% (91 million tonnes) from capture fisheries (FAO, 2024). In terms of aquaculture feed, fishmeal and fish oil are the preferred options due to their high nutritional value and digestibility (Miles & Chapman, 2006). However, since they are primarily sourced from wild-caught fish, their production cannot match the rapid growth of aquaculture without leading to overfishing of marine ecosystems (Matassa et al., 2016). To reduce this pressure, researchers explored alternative and sustainable protein sources, such as plant-based proteins, insect-based proteins, and microbial biomass (Delamare-Deboutteville et al., 2019). Microbial biomass, or single-cell protein (SCP), offers several advantages as a feed ingredient for aquaculture when compared to those derived from plants and insects. Firstly, the conversion of nutrients into proteins is more efficient (Matassa et al., 2016). Secondly, plant and insect-based feeds often contain less digestible and anti-nutritional components, such as cellulose, chitin and phytate, while microbial biomass is highly digestible, well utilized by fish and crustaceans, and has an amino acid profile similar to fishmeal (Gamboa-Delgado & Márquez-Reyes, 2018). Indeed, protein content in bacterial biomass ranges between 50 and 65% (Ravindra, 2000). However, most of microbial SCP production relies on aerobic heterotrophs, which dissipate a substantial fraction of energy during catabolism, limiting biological yields and conversion ratio to below 50% (Matassa et al., 2015). Nevertheless, SCP production costs, even when utilizing waste streams as feedstock, will still be higher than the market price of fishmeal or soybean meal (Alloul et al., 2021). Therefore, added-value properties beyond just the nutritional content of microbial protein should be investigated to increase product value (Alloul et al., 2021). Disease outbreaks represent another major

challenge in aquaculture, often considered a significant bottleneck to animal production and trade (Laranja & Bossier, 2020). The application of antibiotics to control illnesses has, however, brought limited success due to the development of antibiotic resistance, which represents a threat to human and environmental health (Laranja & Bossier, 2020). Given all these considerations, finding alternative strategies that are equally effective and sustainable for mitigating aquaculture diseases, while maintaining optimal nutritional properties, should be the primary focus of research (Laranja & Bossier, 2020).

1.3.1. PPB value in aquaculture

PPB biomass is characterized by high crude protein (CP) contents at around 60% dry weight and a balanced amino acids profile, including high levels of essential amino acids such as cysteine and methionine (Capson-Tojo et al., 2020), which are often added to aquaculture feeds (Candebat et al., 2021). These characteristics enable feed protein substitution for high-value aquaculture species, like salmonids, carnivorous marine fish and shrimp, which require up to 60% of protein in their diets (Jones et al., 2020). Moreover, PPB biomass contains a range of xanthophylls, such as spirilloxanthin, lutein, okenone, spheroidene, and rhodopin, as well as a wide range of carotenes, including lycopene and neurosporene (Sandmann, 2021). These carotenoids, together with BChls, serve as anti-oxidants and play an important role in fish skin and flesh coloration. Indeed, pigments, such as astaxanthin, are added to the diets of salmonids and marine shrimp to improve meat colour (Wade et al., 2017). Vitamins, PHAs, carbohydrates, lipids and minerals are also contained in PPB biomass, highlighting its potential as a single-cell protein source. Furthermore, the biomass can be added directly to aquaculture feed, without requiring any additional extraction costs (Hülsen et al., 2022). The study by Delamare-Deboutteville et al., (2019) is particularly relevant, as it demonstrated that replacing up to 33% of fishmeal with purple non-sulfur bacteria (PNSB) biomass in the feed had little to no impact on the growth performance of Asian sea bass, a species that requires a high dietary protein content. The authors hypothesized that the negative effects of higher inclusion levels might be mitigated through simple pre-treatment methods, such as hydrolysis, which improves digestibility (Delamare-Deboutteville et al., 2019). Moreover, Alloul et al., (2021) investigated the potential of PNSB as an added-value protein ingredient for

shrimp feed. The results showed that PNSB inclusion led to a similar or even enhanced growth performance in shrimp compared to a commercial feed. The authors hypothesized that PNSB might be able to colonize the gastrointestinal tract and assist shrimp digestion, as demonstrated in a study by Chumpol et al., (2018), in which live PNSB actually colonized it and excreted proteases, lipases, and amylases. Additionally, Alloul et al., (2021) showed that the ammonia tolerance of shrimp was even enhanced for shrimp fed with the PNSB *Rhodopseudomonas palustris*, reflecting their added-value potential. In relation to diseases in aquaculture, the application of PHB as a biocontrol agent was first demonstrated in a model crustacean species, *gnotobiotic Artemia*, by Defoirdt et al., (2007). To date, several studies have shown PHB's beneficial effects on aquacultured animals, including improved growth, survival, and robustness against biotic and abiotic stress (Laranja & Bossier, 2020). The growth-enhancing effects of PHB may be linked to its ability to influence the gut microbiota, as demonstrated by De Schryver et al., (2010). In this study, an altered microbial gut composition was found in juvenile seabass fed with a diet containing PHB. These changes appeared to be closely related to the observed increase in fish growth, likely caused by improved nutrient absorption (De Schryver et al., 2010). For feed applications, high PHA accumulation is not required, and the desired inclusion rate ranges from 0.2 to 5 wt% (Santhosh and Umesh, 2021). Indeed, at these concentrations fish and shrimps exhibit increased average weight gain, growth rate, and survival rate (Wang et al., 2019). Mixed and pure PPB cultures are able to produce PHA efficiently. Non-PHA-directed growth already results in approximately 2.5% PHA content within the biomass and, with minimal effort, this content can be increased to a sufficient level to achieve the benefits mentioned above (Hülsen et al., 2022). To explain how PHB or PHA can have beneficial effects in aquacultured animals, it is necessary to examine their chemical composition. PHB can be degraded into β-hydroxybutyric acid, a type of short chain fatty acid (SCFA). SCFAs have antimicrobial properties and they are already used as antimicrobial bio-agents in commercial feed (Hülsen et al., 2022). Particularly in aquaculture, SCFAs demonstrated to inhibit the growth of shrimp pathogens such as *Vibrio campbellii* (Defoirdt et al., 2007). The primary mechanism of pathogen growth inhibition caused by SCFAs is hypothesized to be the undissociated form of the acid, which can easily penetrate the lipid membrane of pathogen through a diffusion process. Once inside the cytoplasm, acid dissociates into anions and protons, lowering the cytoplasmic pH (Eklund, 1983). In order to

maintain neutral pH, the removal of these protons requires active transport, which consumes cellular energy and can lead to lowered cell growth or cell death (Laranja & Bossier, 2020). In addition, SCFAs can damage cell membranes and interfere with numerous processes essential for microorganisms survival (Laranja & Bossier, 2020). However, as SCFAs are water-soluble, their effective delivery to the animal gut can be challenging; moreover, adding SCFAs to the feed can result in significant losses due to leaching, while their direct addition in water necessitates high doses to be effective (Laranja & Bossier, 2020). PHB is the water-insoluble precursor of SCFAs, so it can be easily incorporated in feed or introduced via bioencapsulation method, and delivered in the gut for microbial degradation into SCFAs (Laranja & Bossier, 2020). Indeed, the research of Defoirdt et al., (2007) demonstrated that PHB was about 1000 times more efficient than its monomer form β-hydroxybutyrate. β-hydroxybutyrate can enhance survival and robustness in organisms in three possible ways: by inhibiting the growth or decreasing the virulence of the pathogen, by enhancing the immune response of the animal, and by serving as energy source to the animal (Laranja & Bossier, 2020). Finally, using an analysis of Kyoto Encyclopedia of Genes and Genomes (KEGG) pathways, it has been discovered that genes involved in major metabolic pathways, secondary metabolite biosynthesis, immune system, signalling molecules and interactions are significantly upregulated in organisms fed with PHB-containing feed (Santhosh & Umesh, 2021). As discussed earlier, PHA can exist in an amorphous, intracellular state within living cells and in a partially crystalline state after extraction (Laranja & Bossier, 2020). Amorphous intracellular PHA is naturally bio-encapsulated, allowing effective delivery to gastrointestinal tract, improving feed palatability and minimizing losses through leaching during feeding (Pesante et al., 2022). In literature there are several studies that demonstrate that amorphous PHA is more effective than crystalline PHA. An example is provided by Laranja et al., (2018), whose research showed that the amount of amorphous PHB used to feed *gnotobiotic Artemia* was 82-410 times lower than the suggested effective level of crystalline PHB as indicated by Defoirdt et al., (2007). The higher efficiency of the amorphous biopolymer compared to the crystalline form resulting from extraction can be attributed to its faster degradation (Laranja & Bossier, 2020). Indeed, it has been demonstrated that amorphous PHB can be hydrolyzed 30 times faster than the crystalline form because hydrolytic enzymes can diffuse faster (Yu et al., 2005). To summarize, PPB contain not only PHA but also a range of precious nutrients, including vitamins and pigments, which

can positively contribute to fish growth and health (Alloul et al., 2021). Nevertheless, utilizing waste streams as feed and directly employing the resulting single-cell proteins in aquaculture would eliminate the costs associated with feed supply and the additional costs of extracting valuable components from the harvested biomass (Pesante et al., 2022).

2. Thesis objective

The aim of this thesis is to investigate part of a multi-steps bioprocess mainly focused on the SCP production through the cultivation of PPB, with a feedstock containing wine lees, with the goal of producing PHA-rich biomass, which nutritional value has been preliminary evaluated according to proteins, carbohydrates and lipids content, while valorising a by-product of the wine industry. Specifically, this study examines the effect of organic loading rate (OLR), hydraulic retention time (HRT), and sludge retention time (SRT) on PPB growth, evaluated in a lab-scale 2 L sequencing batch reactor (SBR). Moreover, while most studies in the literature are conducted under sterile and pure culture conditions, or by using a fermented VFA-rich stream, this study employed a mixed microbial culture (MMC) of PPB and unfermented WL (avoiding dark fermentation step) to strongly reduce the overall SCP production cost, which would be higher if a pure and sterile culture were used and if the additional acidogenic fermenter was used. For this purpose, the anaerobic photobioreactor (SBR) containing a mixed microbial culture of PPB was used in three different operating conditions as described in the following chapter. In detail, the specific objectives of this thesis are:

- evaluation of PPB selection and growth on a not fermented ethanol-rich feedstock (WL) as substrate;
- investigation of the OLR on the PPB growth yield in a sequencing batch photobioreactor (SBR);
- quantification of the PHA storage capacity by the PPB from ethanol-rich feedstock;
- evaluation of the PPB nutritional value in a different cultivation condition.

3. Materials and methods

3.1. Mixed microbial culture PPB

The inoculum was obtained by collecting a mixed water and sediment sample from the Sile river. This mixture, after the addition of a fermented carbon source derived from a parallel research activities, was maintained under anaerobic conditions in a photobioreactor and exposed to continuous IR illumination to select and enrich the culture in Purple Phototrophic Bacteria (PPB). As shown in Figure 3, after a couple of weeks the biomass turned to the characteristic dark purple colour of PPB, and the first run began. Throughout all three runs conducted, the biomass maintained the same appearance, with some examples shown in Figure 4.

Figure 3: Biomass after PPB selection and enrichment

a. b. 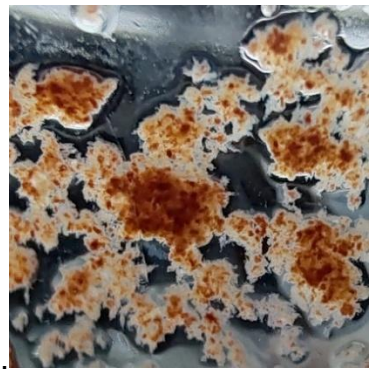 c.

Figure 4: PPB biofilm attached to the photobioreactor wall (a., December 9) and precipitated after the addition of polyamines (b., c., September 27).

For the PPB cultivation, a sequencing batch reactor (SBR) was adopted. The utilized feedstock consisted of wine lees (only the liquid fraction after centrifugation), digestate (from 5 L lab-scale digestor), and tap water in different ratios according to the condition tested, with a cycle length of 12 hours throughout the experimental runs. The anaerobic digestor was fed with a mixture of sewage sludge (from Treviso WWTP) and the solid-rich WL residue. The photobioreactor was continuously illuminated with NIR light (100 W/m^2) to select and enrich the MMC with purple photoheterotrophic bacteria. All three runs were conducted with an HRT of 2 days. In the second run, the OLR was decreased, and in the third run, an SRT different from the HRT was introduced. To clarify, Table 2 summarizes the operating conditions of the three runs.

Table 2: Runs operating conditions

	OLR	**HRT**	**SRT**
	$\frac{gCOD}{L \times d}$	*Day*	*Day*
Run-1	2.74 ± 0.09	2	2
Run-2	1.61 ± 0.04	2	2
Run-3	1.64 ± 0.07	2	4

In particular, in the first condition, an OLR of 2.74 ± 0.09 $\frac{gCOD}{L \times d}$ was used to assess microbial activity and performance in a non-sterile environment at high concentration of ethanol (various and not detected contaminants like polyphenols could influence and impact overall performance). In the second condition, the OLR was reduced to 1.61 ± 0.04 $\frac{gCOD}{L \times d}$. This reduction aimed to enrich the MMC with PPB in a more favourable condition, given the lower COD_{SOL} and ethanol in the media (an excess in COD_{SOL} could compromise the PPB growth in favour of algal contamination). Finally, in the third condition the OLR was similar to second run, with a value of 1.64 ± 0.07 $\frac{gCOD}{L \times d}$, while an SRT of 4 days was applied to investigate the potential improvements in overall performance and nutritional profile attributed to the recirculated biomass. The three runs were conducted in the following periods: June 11 to July 31 (50 days), September 6 to October 21 (45 days), and October 28 to December 9, 2024 (42 days).

3.2. Feedstock preparation

The feedstock was a mixture of wine lees, digestate, and tap water in varying ratios, depending on the target OLR for each run. Red wine lees, provided from a local winery, was collected in different containers and frozen to preserve its nutritional composition. When needed for feedstock preparation, one container at a time was thawed, centrifuged, filtered through 0.45 µm pore size Whatman® glass microfiber filter disc, and stored in the fridge before being used. Digestate was supplied by a lab-scale digester operating in the same laboratory and fed with thickened sewage sludge and solid-rich WL fraction mixture. Table 3 summarizes wine lees and digestate compositions.

Table 3: Wine lees and digestate composition

	pH	TSS	VSS	sCOD	$N\text{-}NH_4^+$	EtOH	OAs (TOT)
		g(TS)/L	*g(VS)L*	*g(COD)/L*	*g/L*	*gCOD/L*	*gCOD/L*
Wine lees	4.68	1.19	0.95	98.75	0.00139	34.035	5.438
Digestate	7.87	0.27	0.215	1.0	0.755	0.0203	0.0225

To compensate for the low level of ammonium ($N\text{-}NH_4^+$) in wine lees, ammonium chloride was externally added to the feedstock to reach a concentration of 0.8 g/L.

3.3. Experimental configuration and cycle schedule

In this study, a 2-liter jacketed glass reactor was used, maintained at a constant temperature of 30°C throughout all three runs. To ensure a homogeneously mixed bacterial culture, a magnetic stirrer was placed inside the reactor, which was positioned on a magnetic stir plate. Moreover, to provide an advantageous environment for PPB growth and enrichment, the reactor was sealed as much as possible to maintain anaerobic conditions and was continuously illuminated by two NIR lamps, with a power of 50 W/m^2 each, positioned 180 degrees apart. Additionally, during the daytime, the

reactor was covered to allow only NIR light exposure, while minimizing sunlight exposure to prevent algae growth, as shown in Figure 5.

Figure 5: Photobioreactor (October 28)

Due to the SBR mode used in this study, both the feeding and the effluent tubes were connected to the reactor, allowing minimal oxygen to enter. Two peristaltic pumps, LLG-uniPERISTALTICPUMP 1 model, were used for the feeding and drawing cycle phases, set to the appropriate rpm to deliver and extract the required volume. In addition, each pump was connected to an individual timer to automate the cycle. A 12-hour cycle was performed twice daily, in the mornings and in the evenings. To achieve an HRT of 2 days, 500 mL of effluent were removed and 500 mL of feedstock were added during each cycle. Both feeding and drawing phases lasted 30 minutes each. This strategy allowed to stabilized the so-called feast-famine condition in the SBR (Montiel-Corona & Buitrón, 2022), with the aim of stimulating the PHA storage response of the PPB. Figure 6A and 6B respectively show the collected effluent stream in a glass cylinder and the reactor appearance during the feeding phase.
For clarity, Table 4 summarizes the SBR cycle schedule used throughout the study.

Table 4: SBR cycle schedule used for all three runs

CYCLE PHASE	VOLUME (*L*)	PHASE LENGHT (*hour*)
Drawing	0.5	0.5
Feeding	0.5	0.5
Photoheterotrophic reaction	2	11

A. 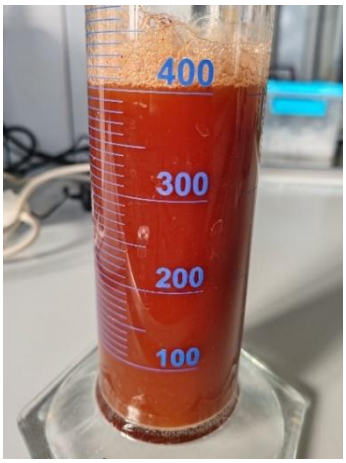

B.

Figure 6: A. Effluent stream (November 8), B. Reactor during feeding phase (October 30)

3.4. Samples preparation

All the analyses were performed three times a week on the effluent stream exiting the reactor after one cycle, shown in Figure 7, and on the freshly prepared feedstock, following the procedure outlined below. Except for the TSS, VSS and PHA analyses, sample was collected in a plastic tube, and pH was measured.

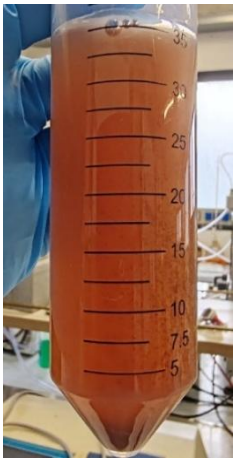

Figure 7: Reactor effluent stream collected in a 50 mL falcon tube before centrifugation (September 6)

After centrifugation at 4000 rpm for 8 minutes, the supernatant was first vacuum-filtered using a 0.45 µm pore size filter disc, and then further filtered using a 0.22 µm pore size syringe filter. Finally, the filtered sample was analyzed for SCFAs, ethanol, sCOD, and ammonium content. Since TSS, VSS and PHA analyses primarily focus on the biomass itself, the method is different. Specifically, for TSS/VSS analysis the sample was collected, properly mixed, and filtered through the filter disc. For PHA analysis, which is performed only on the effluent stream, a fixed amount of properly

mixed sample was placed inside a plastic tube and mixed with a fixed quantity of sodium hypochlorite solution (5% active chlorine).

3.5. Recirculation of the biomass

In the third run, an SRT of 4 days was introduced. To achieve this, all 500 mL of the effluent stream was collected after the first cycle of each weekday and centrifuged at 4000 rpm for 8 minutes. Then, the settled PPB biomass (Figure 8) was collected with a spoon and reintroduced into the photobioreactor.

Figure 8: Centrifuged biomass (November 5)

3.6. Carbohydrate, lipid and protein characterization

To investigate the potential of PPB as SCP source, the carbohydrate, lipid and protein content of the harvested biomass was analyzed in runs 2 and 3. To do so, 500 mL of the effluent stream from each run was collected and centrifuged, then the settled biomass was frozen and lyophilized (Figure 9).

Figure 9: Lyophilized biomass (run-2)

3.7. Analytical methods

3.7.1. SCFAs and ethanol

Short-Chain Fatty Acids (SCFAs) and ethanol were analyzed using an “Agilent 6890N” gas chromatograph equipped with a flame ionization detector (FID) operating at 250°C. The separation was achieved on an Agilent J&W DB-FFAP fused silica capillary column (15 m length, 530 µm diameter, 0.5 µm film thickness). The SCFAs analyzed included acetic, propionic, butyric, valeric and caproic acid. The instrument used hydrogen as carrier and it was programmed with a ramp temperature from 40°C to 160°C, followed by a post-run phase at 220°C. Effluent and feedstock samples for chromatography analysis were prepared in Eppendorf tubes, using 1.0 mL of sample, 100.0 µL of phosphoric acid and 100.0 µL of 2-etilbutyrric acid (internal standard). The qualitative analysis of SCFAs and ethanol was performed by comparing the peak area in the chromatogram to that of the internal standard (2-etilbutyrric acid), which was present in a known concentration. The value obtained were already converted to gCOD/L.

3.7.2. Total solids and volatile solids

Total suspended solids (TSS) represent the total amount of solid material present in a liquid sample, while the volatile suspended solids (VSS) represent the organic matter component within the total solids. For the determination of TSS in effluent and feedstock samples, an aliquot (sample mL) of the homogeneously mixed sample is vacuum-filtered through a pre-weighted (W_0) 0.45 µm pore size filter disc, as shown in Figure 10.

Figure 10: Solids retained on a 0.45 µm pore size filter disc after vacuum filtration of the effluent stream (November 8)

The filter disc, with the retained solids, was then placed in an oven ("Argo lab, TCN115") at 105°C for 48 hours. After drying, the filter disc weight obtained represents the dry residue (W_1). The formula used for the quantification of TS is:

$$TSS\ \left(\frac{g_{TS}}{L}\right) = \frac{W_1\text{-}W_0\ (g)}{sample\ (mL)} \times 1000$$

For the determination of VSS, the dried filter disc is placed in a muffle furnace at 550°C for 24 hours, in order to burn off the organic matter. Then, the filter disc is weighted (W_2) and VSS are calculated by the formula:

$$VSS\ \left(\frac{g_{VSS}}{L}\right) = \frac{W_2\text{-}W_1(g)}{sample\ (mL)} \times 1000$$

In order to estimate the grams of effective biomass recirculated in the third run, a volatile solids (VS) analysis was conducted on the centrifugated biomass. For total solids (TS) determination, an empty crucible was weighed on a technical scale to obtain the tare weight (W_0). A representative quantity of biomass was then weighted into the crucible, obtaining the wet weight (W_1). Following the same procedure as for effluent stream and feedstock sample, the crucible was placed inside the oven at 105°C for 48 hours and then weighted, obtaining the dry residue weight (W_2). TS content was quantified using the formula:

$$TS\ \left(\frac{g_{TS}}{kg}\right) = \frac{W_2\text{-}W_0}{W_1\text{-}W_0} \times 1000$$

For the VS content, the crucible was placed inside the muffle furnace at 550°C for 24 hours and the weighted, obtaining the weight after the incineration (W_3). Finally, VS content was quantified as follow:

$$VS\left(\frac{g_{VS}}{kg}\right) = \frac{W_2\text{-}W}{W_1\text{-}W_0} \times 1000$$

3.7.3. Soluble chemical oxygen demand (sCOD)

The soluble chemical oxygen demand (sCOD) represents the soluble organics present in the liquid phase. This analysis was performed using the colorimetric method with a UV/VIS spectrophotometer. All effluent stream samples were diluted 1:10, while all feedstock samples were diluted 1:25. Subsequently, 2.50 mL aliquots of each diluted

sample was transferred into a pirex glass test tube and an oxidizing solution ($K_2Cr_2O_7$) and a catalyst solution (H_2SO_4) were added to each tube. Thus, the tubes were placed in a digestor ("VelP, Eco16 termoreactor") set at 150°C for a 2-hour digestion period before the spectrophotometric analysis. The sCOD was determined using the sCOD value concentration obtained multiplied by the dilution factor of the sample (D.F), as reported:

$$\text{sCOD}\left(\frac{\text{mgO}_2}{\text{L}}\right) = \text{sCOD}_{\text{measured}}\left(\frac{\text{mgO}_2}{\text{L}}\right) \times \text{D.F.}$$

3.7.4. Ammonium analysis

To determine the concentration of ammonium ions (NH_4^+) in samples, an ammonium probe was used. This analytical instrument operates on the principle of potentiometry, employing a selective membrane for ammonium ions. When immersed in a solution containing NH_4^+, a potential difference is established between the inside and outside of the membrane, proportional to the concentration of ammonium ions in the solution. This potential difference is measured by a voltmeter and converted into NH_4^+ concentration through a calibration curve. Five 10 mL each standard solutions with an increased NH_4^+ concentration (10^{-1} M, 10^{-2} M, 10^{-3} M, 10^{-4} M, 10^{-5} M) were prepared. The probe was immersed in each solution to measure the potential, allowing for the construction of the calibration curve. Then, the probe was immersed in 10 mL of filtered effluent and feedstock samples, 1:2 diluted, and the measured potential value was interpolated on the calibration curve to obtain the NH_4^+ concentration. All standard solutions and samples were analyzed in a beaker agitated by a magnetic stirrer. To ensure accurate and reliable measurements, 200 microliter of ISA buffer solution were added to each, in order to maintain a constant ionic strength and to optimize the pH of the samples.

3.7.5. PHA analysis

PHA analysis was conducted on effluent stream samples exiting the photobioreactor. 5 mL of each sample was pre-treated with 1.0 mL of sodium hypochlorite solution (5% active chlorine) in a plastic tube, in order to lyse PPB cells and release intracellular

PHA. After shaking, tubes were stored at -20°C. PHA quantification was performed using gas chromatography based on acid methanolysis. In this method, acidified methanol (3% v/v H_2SO_4) solution was used to hydrolyze PHA, converting it into its corresponding methyl esters methyl-3-hydroxybytyrate (3HB) and methyl-3-hydroxyvalarate (3HV). For sample preparation, frozen samples were thawed and centrifuged at 4700 rpm for 20 minutes, resulting in the sedimentation of the biomass, as shown in Figure 11.

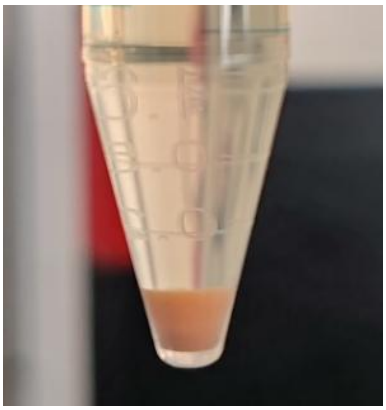

Figure 11: Settled biomass after centrifugation (December 2)

The supernatant was discarded, and the solid residue was quantitatively transferred into pyrex glass tubes containing 2.0 mL of acidified methanol solution with 0.05 g/L benzoic acid as internal standard. Then, 1.0 mL of chloroform was added, and the mixture was digested at 100°C for 4 hours using a “Velp Eco16 thermoreactor” digester. After cooling, 1.0 mL of distilled water was added and tubes were mixed thoroughly, finally resulting in the formation of two distinct phases: aqueous and organic. 1 µL of the organic phase was directly injected into the same gas chromatograph used for SCFAs and ethanol analyses, which used a run temperature from 100°C to 130°C, and a post-run phase at 240°C. Quantitative determination of poly(HB/HV) was carried out by constructing calibration curves for HB and HV, both with zero intercepts. Calibration standards were prepared using poly(HB/HV) copolymer from Aldrich, containing 95% HB and 5% HV by weight. The sample preparation procedure for standards was identical to that for the samples, except for the centrifugation step. Results, expressed in mg/L, were converted to $\left(\frac{\text{mgCOD}}{\text{L}}\right)$ using theoretical factors of 1.67 and 1.91 $\left(\frac{\text{gCOD}}{\text{gPHA}}\right)$ for HB and HV respectively, based on complete oxidation of each monomer. The polymer content within the biomass was

determined by dividing the polymer concentration $\left(\frac{\text{mgPHA}}{\text{L}}\right)$ by the total biomass concentration $\left(\frac{\text{mgVSS}}{\text{L}}\right)$, as shown:

$$\text{Polymer content } \left(\frac{\text{mgPHA}}{\text{mgVSS}}\right) = \frac{\text{Polymer concentration } \left(\frac{\text{mgPHA}}{\text{L}}\right)}{\text{Biomass concentration } \left(\frac{\text{mgVSS}}{\text{L}}\right)}$$

3.7.6. Carbohydrates, lipids and proteins content

For carbohydrates, lipids and proteins content, spectrophotometric methods were used. The carbohydrate content was assessed using the phenol-sulfuric acid method, a simple and rapid colorimetric technique for quantifying total carbohydrate in a sample. Concentrated sulphuric acid hydrolyzes complex carbohydrates into their constituent monosaccharides pentoses and hexoses. Subsequently, these monosaccharides undergo dehydration, forming furfural and hydroxymethylfurfural, respectively. These compounds then react with phenol, producing a characteristic yellow-gold colour that is quantified using a UV-Vis spectrophotometer. Firstly, a 72% sulfuric acid solution and a 5% phenol solution were prepared. Then, 0.01 g of lyophilized biomass was weighed and dissolved in 10 mL of distilled water. 1 mL of this solution was transferred to a glass tube, and 3 mL of 72% sulfuric acid and 1 mL of 5% phenol were added. The mixture was incubated in a water bath at 90°C for 5 minutes, and after cooling, the absorbance at 490 nm was read. Using a calibration curve constructed with glucose solutions at various concentrations, the carbohydrate content in the sample was determined. The lipid content was assessed using the phospho-vanillin method. For reagent preparation, 0.3 g of vanillin was weighed and dissolved in 50 mL of a 45:5 (v/v) mixture of Milli-Q water and ethanol. Then, 200 mL of phosphoric acid was added carefully, and the solution was stored at 4°C until use. For lipid analysis, 0.002 g of lyophilized biomass sample was weighed and dissolved in 1 mL of distilled water, and 100 µL of this was transferred into a suitable tube. Then, 2 mL of 98% sulfuric acid was added, the mixture was thoroughly mixed and then heated at 100°C for 10 minutes. After cooling in ice for 5 minutes, 5 mL of phosphovanillin reagent was added, and the mixture was mixed again. It was then incubated at 40°C for 15 minutes, with shaking every 5 minutes. The mixture was then kept at room

temperature in the dark for 45 minutes, and after the absorbance at 530 nm was measured. Using a calibration curve, the lipid concentration of the sample was determined. Protein content was determined using the Bradford assay, a rapid procedure for quantifying total protein concentration in a sample. This assay relies on the colorimetric shift of Coomassie Brilliant Blue G-250 dye from 465 nm to 595 nm when it binds to proteins. This shift is driven by hydrophobic and ionic interactions that stabilize the dye's anionic form. Within the assay's linear range, typically 5-25 µg/ml, protein concentration is directly proportional to the dye binding and the resulting increase in absorbance. 0.01 g of lyophilized biomass was added to 10 mL of 0.5M NaOH solution in a clean tube, which was then placed in a water bath at 80°C for 10 minutes. Subsequently, the mixture was centrifuged at 3900 rpm for 20 minutes, and the supernatant was transferred to a clean tube. Then, 2 mL of Bradford reagent was added to 40 µL of the supernatant and 1960 µL of distilled water. The mixture was mixed by inverting and kept at room temperature for 10 minutes, then the absorbance of the sample was read at 595 nm. The protein concentration of the sample was determined by comparing its absorbance to a standard curve generated using known protein concentrations samples.

3.8. Calculations

The OLR was calculated as follows:

$$\text{OLR} = \frac{\left[\left(\text{gCOD}_{\text{EtOH}}/\text{d}\right) + \left(\text{gCOD}_{\text{OAs}}/\text{d}\right)\right] \text{ feedstock}}{\text{Reactor volume}}$$

The PPB biomass productivity was calculated as follows:

$$\text{PPB productivity} = \frac{\text{gVSS/d}}{\text{Volume reactor}}$$

The percentage of PHA contained within the biomass was calculated as follows:

$$\%\text{PHA} = \frac{\text{gPHA/L}}{\text{gVSS/L}} \times 100$$

The active biomass was calculated as follows:

$$X_A = \left(\text{gVSS/L}\right) - \left(\text{gPHA/L}\right)$$

The $COD_{removed}$ was calculated as:

$$gCOD/L_{removed} = \left(\frac{gCOD_{EtOH+OAs}}{L}\right) \text{feedstock} - \left(\frac{gCOD_{EtOH+OAs}}{L}\right) \text{effluent stream}$$

The PHA production yield was calculated as follows:

$$Y_{PHA/S} = \frac{gCOD_{PHA}/L}{gCOD_{removed}/L}$$

A clarification is necessary: since the PHA concentration was measured 4 hours after the feeding phase of a cycle, while the COD removed was calculated 12 hours after that, the PHA storage yield was underestimated. In fact, after the first 4 hours post-feeding, the COD consumed was no longer used for PHA synthesis. As a result, the COD removed at the end of the cycle was higher, and since it appears in the denominator of the formula, it led to a decrease in the storage efficiency calculation.
The observed yield in the SBR was calculated as follows:

$$Y_{OBS}^{SBR} = \frac{(gCOD_{X_A}/L) + (gCOD_{PHA}/L)}{gCOD_{removed}/L}$$

Where

$$gCOD_{X_A}/L = \frac{gX_A}{L} \times 1.42$$

given that the conversion factor for biomass to COD is 1.42.

4. Results and discussion

4.1 Photobioreactor operation: Run–1

4.1.1 Feedstock characterisation

In the first run, an HRT of 2 days and an OLR of 2.74 ± 0.09 $\frac{\text{g COD}}{\text{L×d}}$ were used to evaluate microbial activity and performance in a non-sterile environment, where the presence of different contaminants could influence the overall performance. One liter of feedstock was composed of 300 mL of digestate (necessary for micronutrients supply), 150 mL of wine lees and 550 mL of tap water. To compensate for the low ammonium concentration in the feedstock, primarily caused by the low levels in wine lees, ammonium chloride was added externally to achieve an average concentration of 0.180 g $N\text{-}NH_4^+$/L approximately. Table 5 summarizes the average values of the relevant characteristics of the feedstock used in this run.

Table 5: Feedstock characterisation – Run-1

pH	**TSS**	**VSS**	**COD_{SOL}**	**$N\text{-}NH_4^+$**	**EtOH**	**OAs (TOT)**	**$\frac{\text{OAs+EtOH}}{COD_{SOL}}$**
	g(TS)/L	*g(VS)/L*	*g(COD)/L*	*g/L*	*gCOD/L*	*gCOD/L*	*COD/COD %*
6.57 ± 0.07	0.20 ± 0.03	0.18 ± 0.02	6.93 ± 0.03	0.18 ± 0.04	3.8 ± 0.1	1.6 ± 0.1	80 ± 3

Since both wine lees and digestate were filtered through a 0.45 µm glass-fiber filters before being used, the VSS value was low, even though not negligible (<0.2 g VSS/L). Both ethanol (EtOH) and total organic acids (OAs) contribute to the soluble COD (COD_{SOL}) concentration in the feed, and their sum represents its identified portion. Given that wine lees also contains organic compounds with high molecular weight, such as polyphenols and tannins (Devesa-Rey et al., 2011) the ratio between this sum and the COD_{SOL} value, which is determined by the spectrophotometric method, is an important parameter for assessing the percentage of identified COD_{SOL}. Regarding the organic acids that was detected in the feedstock, Figure 12 illustrates the percentage

distribution of the substrates identified in the feedstock. Ethanol was the most abundant component, while organic acids accounted for approximately 30%, with propionic acid being slightly more prevalent than acetic acid, and only a minimal contribution of butyric acid.

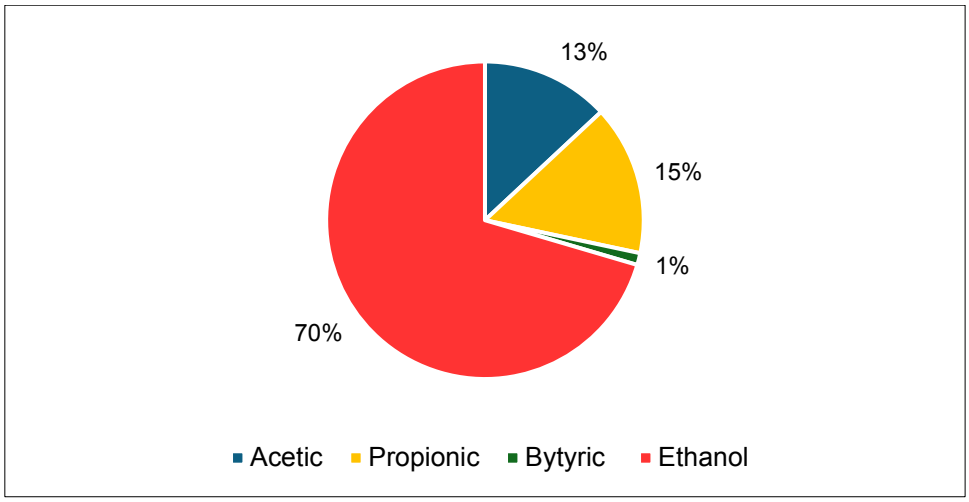

Figure 12: Organic acids profile in the feedstock – Run-1

As shown in Figure 13, the OLR trend over time remained relatively stable, ranging from 2.13 to 3.05 $\frac{\text{g COD}}{\text{L}\times\text{d}}$. Given that the feedstock consisted of a mixture of real waste streams rather than a synthetic medium, the variability in OLR values can be partially controlled by changing dilution factor of carbon-rich feedstock. Synthetic feedstock are usually not subjected to such variability and represent the best option to work in a controlled conditions. However, lab-scale systems with synthetic feedstock do not describe close-to-reality working conditions. For this reason, it has been decided to maintain the same dilution factor for the whole run, accepting some variability in the nutrients' load, and, in turn, describing working conditions close to the real environment. In the days where the OLR value was not reported, the utilized feedstock was previously prepared and the related OLR value was the closer, located before. On average, the feedstock was prepared once per week. Nevertheless, by using the same protocol for feedstock preparation, the OLR was effectively controlled throughout the experiments.

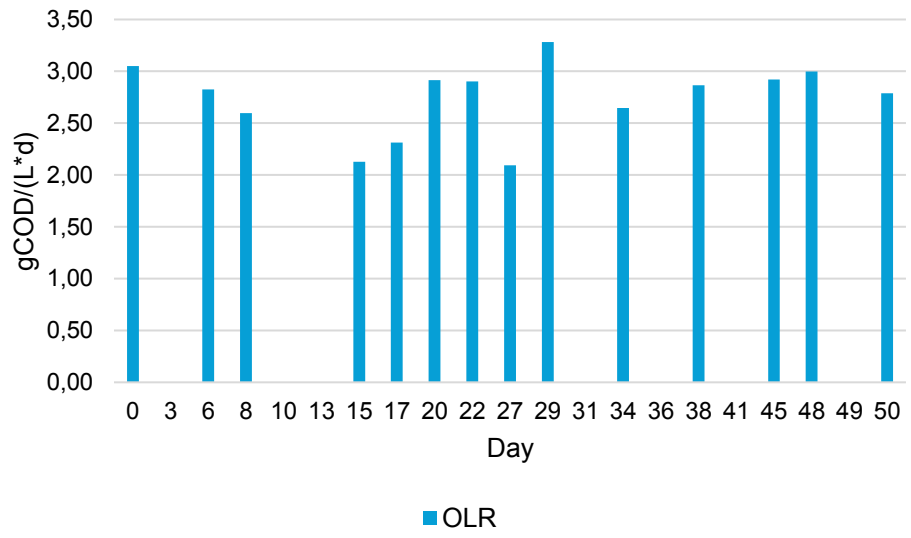

Figure 13: OLR trend – Run-1

4.1.2 Photobioreactor performances

For all three runs, the effluent stream from the photobioreactor was analyzed for VSS, TSS, COD_{SOL}, ethanol, OAs (tot), N-NH_4^+ and biopolymers content, and pH. In this first run, the stability phase was observed from day 8, after an initial period of biomass adaptation. Since the production of SCP is one of the primary objectives of this thesis, the VSS content is a key parameter. Figure 14 represents the trends of TSS and VSS over time. Two main fluctuations are evident: one during the first week, likely due to the assessment of the PPB biomass to a relatively short HRT and relatively high OLR, and one after the midpoint of the test period. Conversely, the trends in the last five days were stable. Columns in the figure represent the VSS/TSS ratio, which indicates the fraction of the solids that consisted of organic materials, such as cells. This ratio had an average value of 0.91 ± 0.02, suggesting that the large majority of the solids exiting the reactor were cells. Overall, TSS and VSS trends appeared with several but not intensive fluctuations from one day to the next. Finally, the PPB biomass productivity had an average value of 0.54 ± 0.03 $\frac{g\ VSS}{L \times d}$.

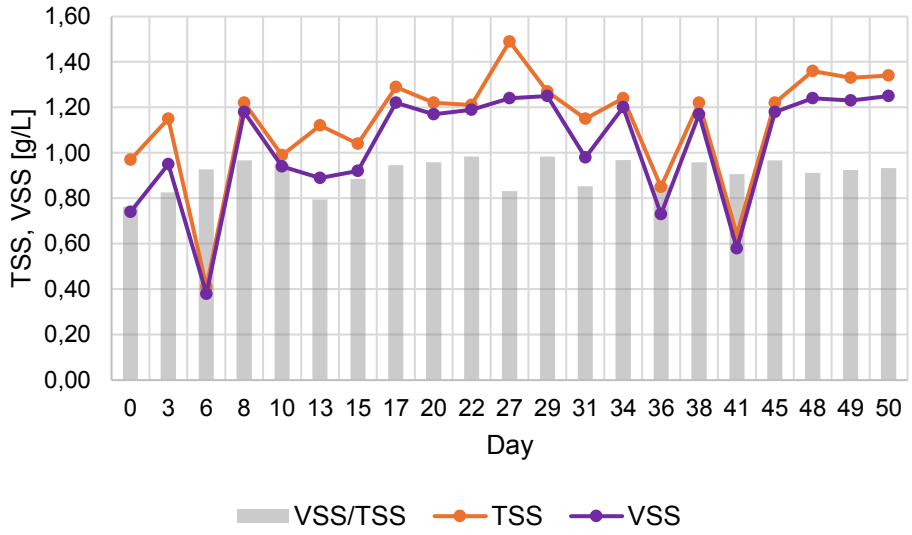

Figure 14: TSS, VSS and VSS/TSS trend – Run-1

Although ethanol is an interesting substrate, it is a particularly complex compound for biological conversion processes (Montiel-Corona & Buitrón, 2022). Firstly, unlike glucose or acetic acid, its assimilation is not as immediate, and secondly, it can inhibit cell growth above a certain threshold. This implies that ethanol assimilation does not occur as rapidly and easily as with other more common substrates. In fact, the majority of studies on PPB cultivation focuses on using feedstocks containing VFAs as primary growth substrates, which are directly assimilable energy sources for microorganisms, while the use of feedstocks rich in unfermented ethanol is still under exploration. Figure 15 illustrates the trends of COD_{SOL}, ethanol and total organic acids (OAs tot) in both the feedstock and the effluent stream exiting the reactor over time. As shown in the graph, a critical point is the presence of residual ethanol in the effluent. OAs_{TOT} were almost totally consumed, with an average removal rate of 96 ± 3% and an average concentration of 0.041 ± 0.01 gCOD/L, suggesting the straightforward assimilation of these substrates. Moreover, the only organic acid detected in the effluent stream was acetic acid, indicating that propionic and butyric acids were completely consumed. Conversely, ethanol concentration was 1.6 ± 0.1 gCOD/L, with an average removal rate of 59 ± 4%. The presence of about 40% of untreated ethanol in the effluent may seems like a negative aspect, but since the aim of this study is to conduct a productive process and not a depurative one, the primary goal is not to achieve a low substrate concentration into the effluent stream, but rather to maximize biomass productivity. If the ethanol were too low the reaction kinetics would inevitably be lower, and the

biomass would grow under substrate limitation conditions, resulting in reduced productivity and requiring an increase in the reactor volume. Although the residual ethanol in the effluent requires further treatment and valorization, maintaining an adequate concentration of ethanol in the feedstock helps avoid biomass growth rate limitations. Regarding COD_{SOL}, the average value in the effluent is 3.4 ± 0.3 gCOD/L, with an average removal rate of 50 ± 5%. As discussed earlier, around 80% of the COD_{SOL} in the feedstock was represented by the sum of ethanol and total organic acids, so this high residual value was likely derived from the residual ethanol concentration in the effluent stream and the unidentified COD_{SOL} portion. In summary, the process showed positive characteristics, with high efficiency in the OAs removal and interesting biomass productivity, despite the presence of residual ethanol, a relatively high OLR for a phototrophic biomass-based process, and a quite low HRT.

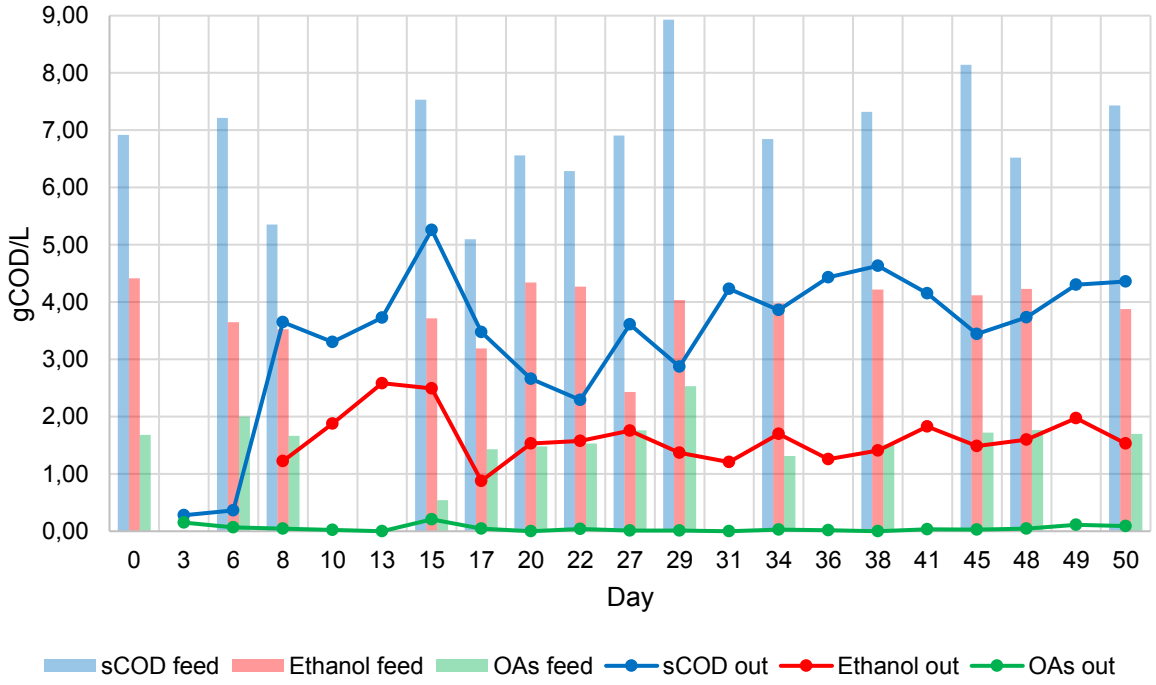

Figure 15: COD_{SOL}, Ethanol and OAs_{TOT} trend – Run-1

Figure 16 illustrates the trends in pH and ammonium concentration in the reactor effluent. A noticeable increase in pH was observed in both the initial and final stages of the experiment, which can be attributed to the possible occurrence of a basic hydrolysis reaction. In fact, the high consumption rate of OAs generated basic hydrolysis reaction, which caused the pH to rise (Montiel-Corona & Buitrón, 2022). Regarding ammonium concentration, its average value was 1.9 ± 0.8 mg/L, with a

removal rate of 96 ± 0.5%. Since nitrate production from ammonium can be excluded in an anaerobic environment, as in this study, it can be concluded that all the ammonium was assimilated for cellular growth.

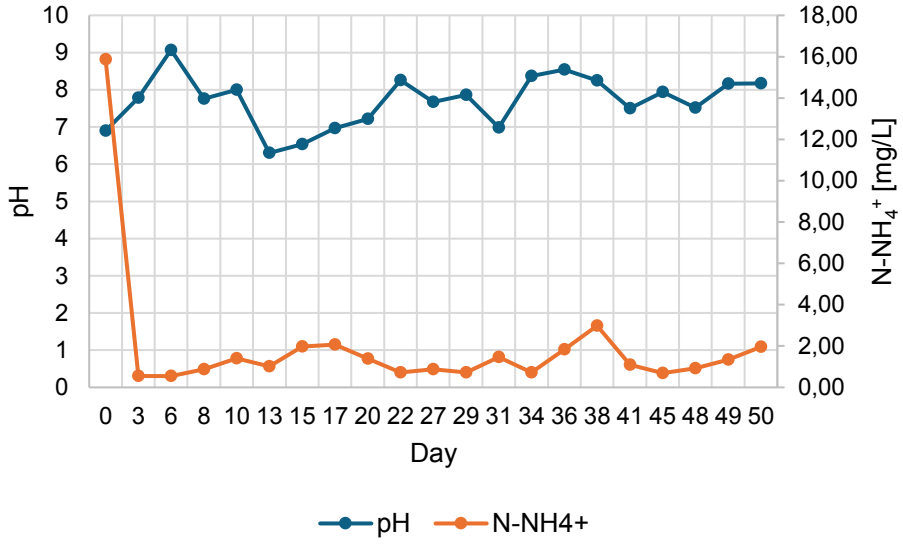

Figure 16: pH and N-NH_4^+ trend – Run-1

A stable PHA production was observed within the stability period, as shown in Figure 17. PHA concentration, with an average value of 102 ± 6 mg/L, was the sum of P(3)HB (poly-3-hydroxybutyrate) and P(3)HV (poly-3-hydroxyvalerate). P(3)HB was the main biopolymer produced, with an average value of 73 ± 4 mg/L. The average concentration of P(3)HV was 30 ± 2 mg/L, lower than that of P(3)HB, but not negligible. The biopolymers percentage can be seen in Figure 18. The difference in the types of biopolymer produced is according to the different metabolic pathways for the consumption of ethanol and organic acids.

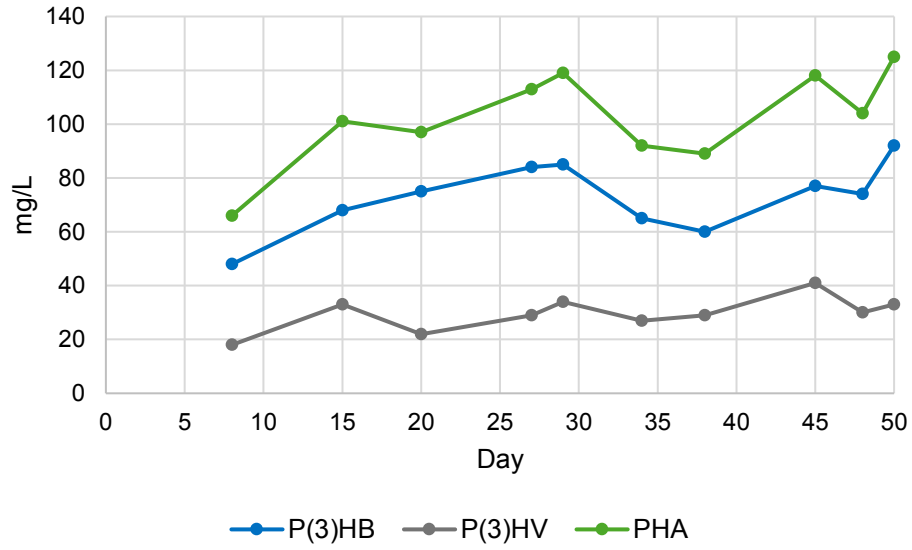

Figure 17: Biopolymers trend – Run-1

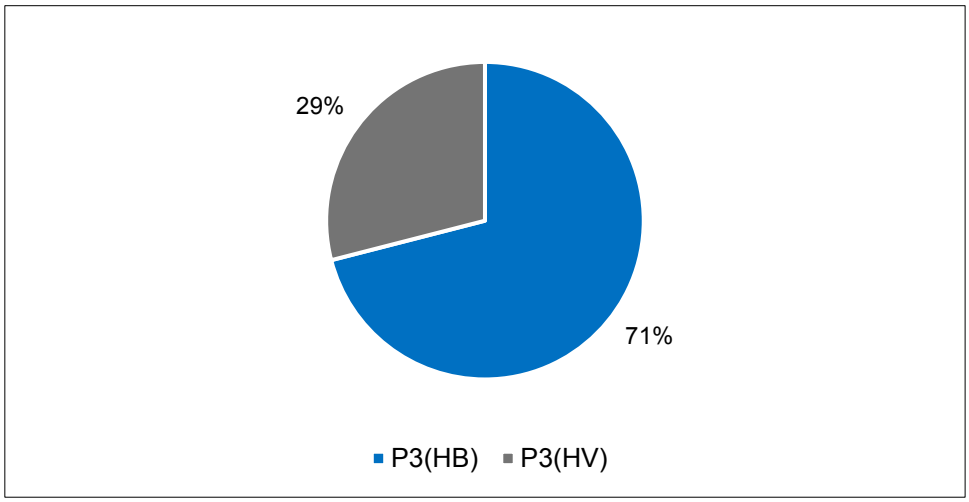

Figure 18: PHB and PHV percentage (wt%) – Run-1

In Figure 19, the trends of active biomass (X_A), produced PHA and ethanol are observed. The active biomass represents the portion of the biomass involved in growth and metabolism without producing PHA. As previously discussed, thanks to the great PPB metabolism, PHA accumulation does not require feast famine selection, allowing both biomass growth and PHA production (Capson-Tojo et al., 2020). This indicates that, under continuous feast conditions as in this study, biopolymer production was closely linked to biomass growth (Montiel-Corona & Buitrón, 2022). Moreover, it can be seen in the figure that when the ethanol concentration in the reactor exceeded or was equal to 1.5 gCOD/L, it likely caused stress in the biomass, leading to increased PHA production, as observed on day 15, 27, 45 and 50. Looking at the trends, ethanol

seemed to inhibit biomass growth beyond a certain concentration, while stimulating PHA production. In fact, ethanol appears to act as a stress-inducing agent for microorganisms, thereby promoting PHA production (Montiel-Corona & Buitrón, 2022).

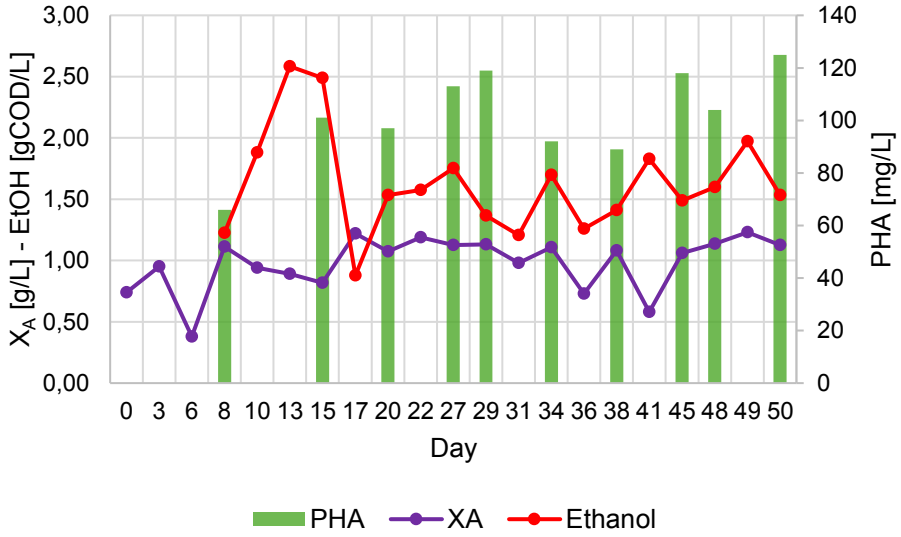

Figure 19: Active biomass, Ethanol and PHA trend - Run-1

For all three runs, the PHA value considered was the one contained within the biomass sampled from the reactor 4 hours after the start of the cycle, and it closely corresponds to the maximum achievable value determined by previous intracycle analyses carried out in parallel, which are not included in the objectives of this study.

The average values of these parameters are summarizes in Table 6. Regarding the observed biomass yield, the value was consistent with literature, which indicates a biomass yield ranging from 0.2 to 0.7 $COD/COD_{removed}$ when grown on a waste carbon substrates, as in this study. Additionally, literature suggests that acetate is the most suitable carbon source, giving a biomass yield up to 1 $COD/COD_{removed}$. In this run, acetic acid accounted for only 44% of the OAs_{TOT}, which may have contributed to the low observed biomass yield (Rashid et al., 2024).

Table 6: Active biomass concentration, %PHA, PHA and observed yields – Run-1

X_A	$Y_{PHA/S}^{feast}$	%PHA	Y_{OBS}^{SBR}
g/L	*$COD/COD_{removed}$*	*g/g_{VSS}*	*$COD/COD_{removed}$*
0.98 ± 0.06	0.05 ± 0.01	8.7 ± 0.5	0.33 ± 0.02

4.2 Photobioreactor operation: Run–2

4.2.1 Feedstock characterisation

In the second run, a reduced OLR of 1.61 ± 0.04 $\frac{gCOD}{L \times d}$ was used, aiming to enrich the MMC with PPB while minimizing algal contamination, which allowed subsequent quantification of carbohydrates, lipids, and proteins content in the harvested biomass. One liter of feedstock contained 150 mL of digestate, 80 mL of wine lees, and 770 mL of tap water. Similarly to run-1, ammonium chloride was externally added to compensate for the low ammonium levels in the feedstock, in order to achieve an average concentration of 0.18 ± 0.04 g/L. Average values of the most relevant feedstock characteristics are summarized in Table 7.

Table 7: Feedstock characterisation – Run-2

pH	**TSS**	**VSS**	**COD_{SOL}**	**N-NH_4^+**	**EtOH**	**OAs (TOT)**	**$\frac{OAs+EtOH}{COD_{SOL}}$**
	g(TS)/L	*g(VS)/L*	*g(COD)/L*	*g/L*	*gCOD/L*	*gCOD/L*	*COD/COD %*
6.57 ± 0.08	0.18 ± 0.02	0.17 ± 0.03	3.9 ± 0.1	0.18 ± 0.04	2.57 ± 0.07	0.65 ± 0.04	83 ± 2

The pH value remained consistent with that of the first run, indicating no variations in the acidity and neutrality conditions of the feedstock. Similarly, the TSS and VSS values remained within the same range, with a slight reduction in the TSS content. With a reduced OLR, lower concentrations of COD_{SOL}, ethanol and total organic acids were observed, while the percentage of identified COD_{SOL} slightly increased but remained within the same range as in run-1. Figure 20 illustrates the percentage distribution of the chemical components detected in the feedstock. Compared to run-1, the ethanol percentage increased up to 80%, while organic acids accounted for 20% of the total. In this run, acetic acid was slightly more abundant than propionic acid, with a minimal contribution of butyric acid.

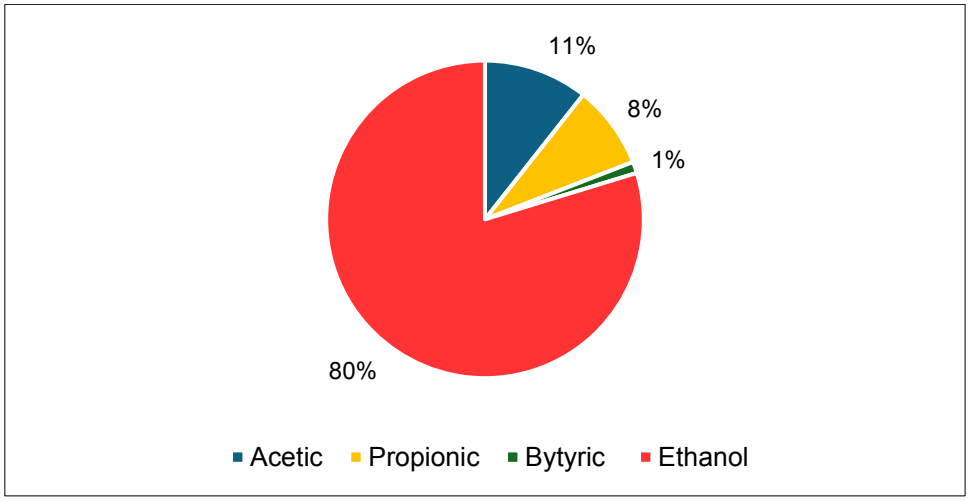

Figure 20: Organic acids profile in feedstock – Run-2

The temporal trend of the OLR is shown in Figure 21. Compared to run-1, this run exhibited more stable values, despite some fluctuations caused by the use of real waste streams, which naturally led to variations in the chemical composition of the feedstock, as previously explained. Fluctuations were less pronounced up to day 26, while more significant variations occurred between days 33 and 40. Nevertheless, the OLR was effectively controlled throughout the entire experiment.

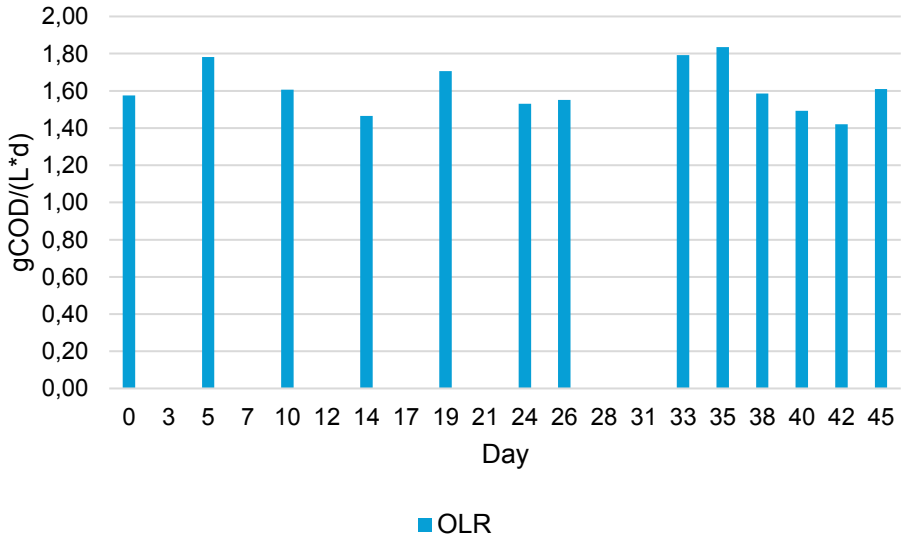

Figure 21: OLR trend – Run-2

4.2.2 Photobioreactor performances

The stability phase began on day 5, after an initial period of biomass adaptation to the reduced OLR. Figure 22 illustrates the temporal trends of TSS and VSS concentrations in the reactor effluent. The TSS average value was 0.93 ± 0.03 g/L, while the VSS average value was 0.84 ± 0.03 g/L. During the first five days, a marked decrease in VSS concentration was observed, dropping from an initial value of 1.24 g/L, which was very close to the final VSS value recorded in run-1 (1.25 g/L), likely due to biomass adaptation to the reduced OLR. The VSS trend was particularly stable during two periods: from day 5 to day 12, and from day 33 to day 45. Between these periods, fluctuations were observed, with VSS value ranging from a minimum of 0.72 g/L to a maximum of 0.94 g/L. The TSS trend generally followed that of the VSS, with the exception of day 35, when a discrepancy between TSS and VSS was noted. Equally to run-1, the VSS/TSS ratio had an average value of 0.91 ± 0.02, suggesting that the large majority of solids in the reactor were cells. The substantial OLR reduction likely led to decreased nutrient availability, reducing biomass growth rate and, consequently, resulting in a lower VSS concentration. In particular, the biomass productivity had an average value of 0.42 ± 0.01 $\frac{\text{g VSS}}{\text{L}\times\text{d}}$, lower than that in the first run. Overall, the reduced OLR led to less fluctuations in VSS concentration in the reactor, indicating a more stable process and more uniform biomass growth.

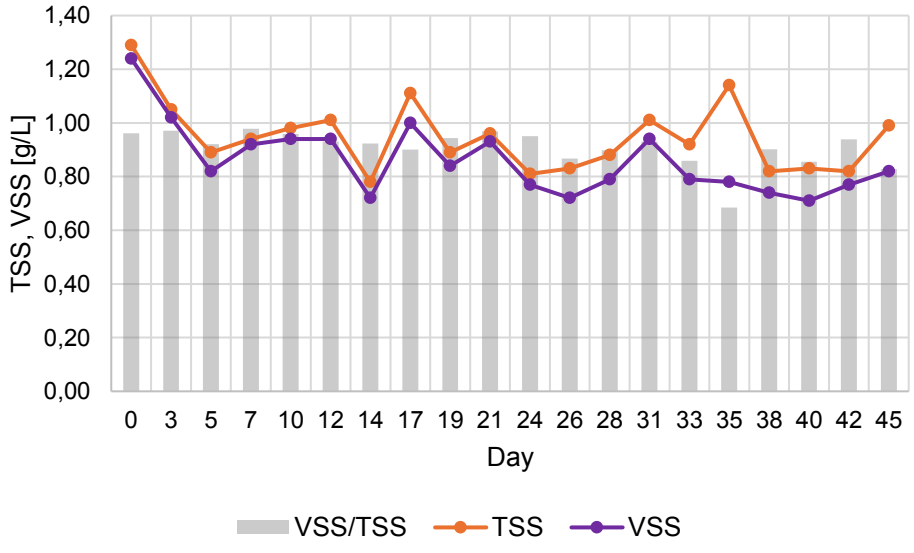

Figure 22: TSS and VSS trend – Run-2

Figure 23 illustrates the temporal trends of COD_{SOL}, ethanol and total organic acids in both the feedstock and the reactor effluent. A residual average ethanol concentration of 1.24 ± 0.07 gCOD/L was detected in the effluent stream, along with an average COD_{SOL} value of 2.21 ± 0.09 gCOD/L. Although these values were lower than those recorded in the first run, the substrates removal efficiencies decreased, with an ethanol removal rate of 54 ± 2 % and a COD_{SOL} removal rate of 43 ± 4%. These results were in line with the reduced biomass productivity caused by the reduction in OLR. As previously mentioned regarding the residual ethanol in run-1, the reduced OLR resulted in a lower substrate concentration, which may have become limiting, thereby slowing the kinetics. Similarly, OAs_{TOT} in the effluent stream had an average concentration of 0.09 ± 0.01 g/L, which was higher than that in run-1, while the average removal rate was 83 ± 3 %, lower than that of run-1. In summary, the reduction in OLR did not result in an improvement in substrate removal.

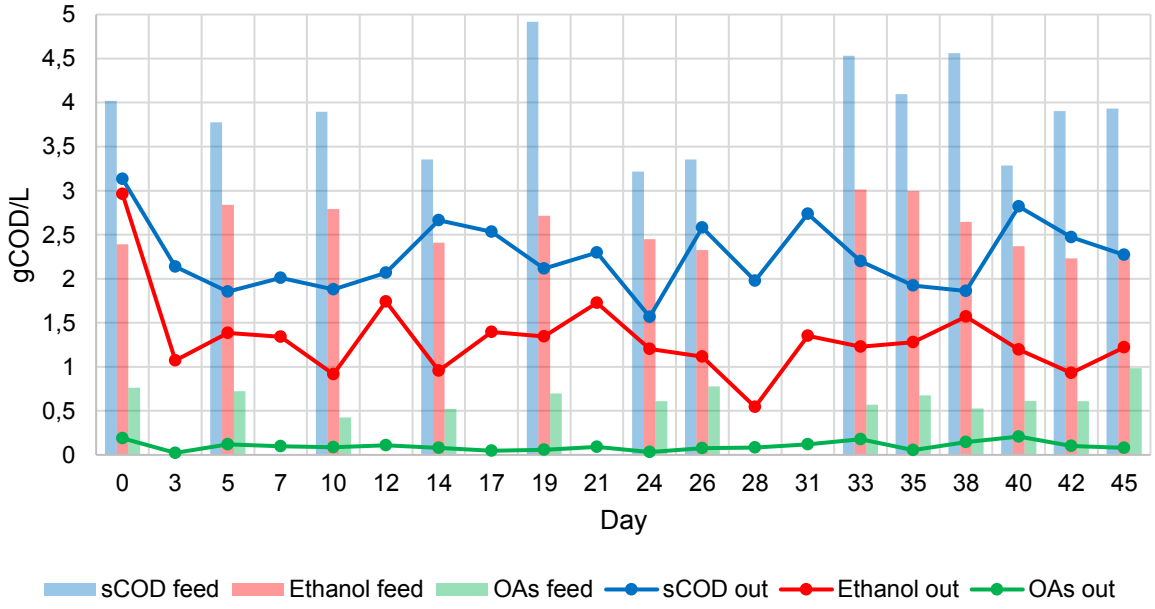

Figure 23: COD_{SOL}, Ethanol and OAs_{TOT} trend – Run-2

Figure 24 presents the temporal trends of pH and ammonium concentration in the effluent stream. During the stability period, the pH exhibited a more stable and consistent trend compared to run-1, with a lowered average value of 6.1 ± 0.2. This reduction may have been associated with slightly less efficient ethanol and OAs removal, which could have contributed to a more acidic environment. Regarding ammonium concentration, the average concentration was 1.1 ± 0.2 mg/L, slightly lower

than that in run-1, with an average removal of 96 ± 1%. As for run-1, since the environment was anaerobic, the available ammonium was entirely utilized for biomass growth.

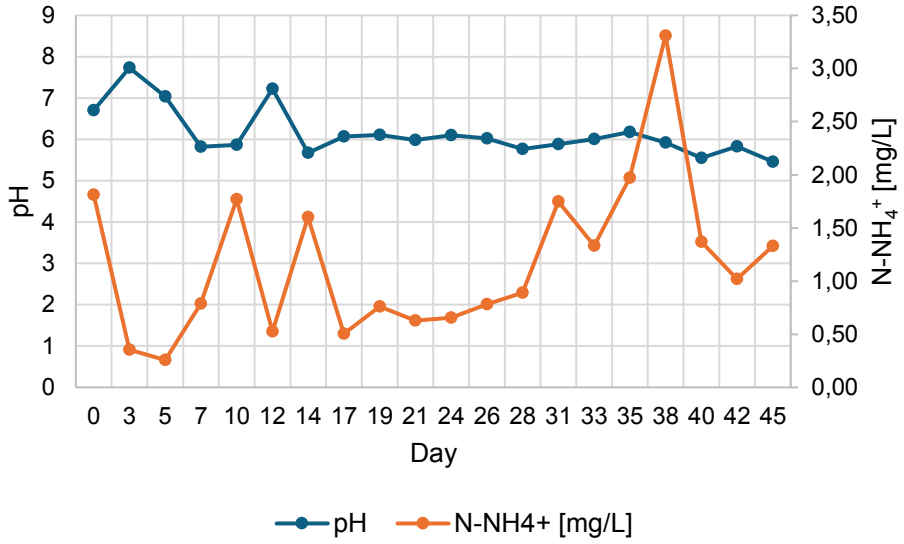

Figure 24: pH and N-NH_4^+ trend – Run-2

Regarding biopolymer concentration, its temporal trend is shown in Figure 25. PHA concentration increased compared to run-1, with an average value of 75 ± 5 mg/L. As in run-1, P(3)HB was the predominant biopolymer produced (average concentration of 63 ± 4 mg/L), with a minimal synthesis of P(3)HV (average concentration of 12 ± 3 mg/L), which percentage (wt%) can be seen in Figure 26. However, the trends exhibited significant fluctuations and could not be considered stable. Nevertheless, polymers production was consistently observed starting from the stability period.

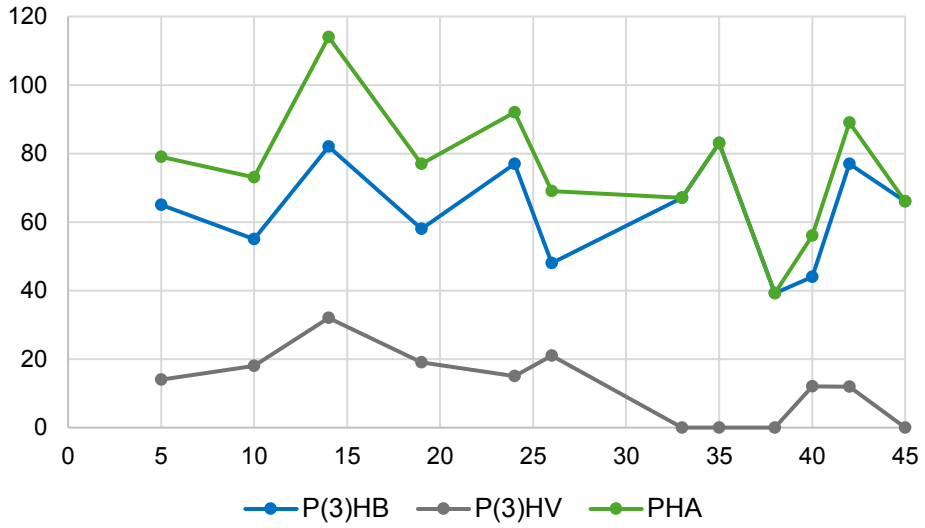

Figure 25: Biopolymers trend – Run-2

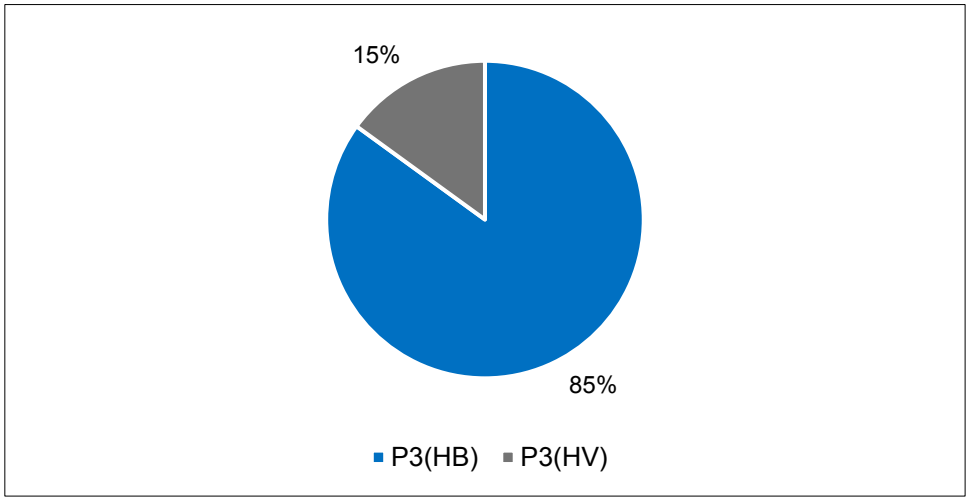

Figure 26: PHB and PHV percentage (wt%) – Run-2

The X_A, PHA and ethanol trends in the reactor effluent are represented in Figure 27. The X_A trend was relatively stable over time, while PHA trends showed some fluctuations. This was likely due to the reduction in OLR while maintaining the same HRT, which resulted in relatively low availability of readily biodegradable substrates for cells, leading to a certain fluctuation in the PHA production capacity. When the most significant fluctuation in ethanol concentration in the reactor effluent occurred (such as on days 12, 21, 28 and 31), no PHA concentration data were available, making it impossible to determine whether the ethanol fluctuations caused an increase or decrease in PHA production. However, on day 14, a decrease in ethanol concentration in the reactor was observed, along with a significant increase in PHA concentration, suggesting that ethanol was utilized for PHA production. In this run, the ethanol

concentration reached a maximum of 1.74 gCOD/L on day 12, so no stress due to high ethanol concentration was observed, as seen in run-1. Conversely, since ethanol was the primary nutrient in the feedstock, it served as a substrate for PHA accumulation rather than a stressor. As evidence of this, in the last 10 days, with a stable trend of X_A, the increase in ethanol on day 38 resulted in a decrease in PHA concentration, indicating that ethanol was not used for biopolymer synthesis. Meanwhile, on day 42, the decrease in ethanol and the increase in PHA suggest that ethanol was used for its synthesis. According to data, it was difficult to quantify the ethanol fraction converted to PHA, but, even under this process condition, the PHA represented a product of the complex metabolic pathways of purple bacteria.

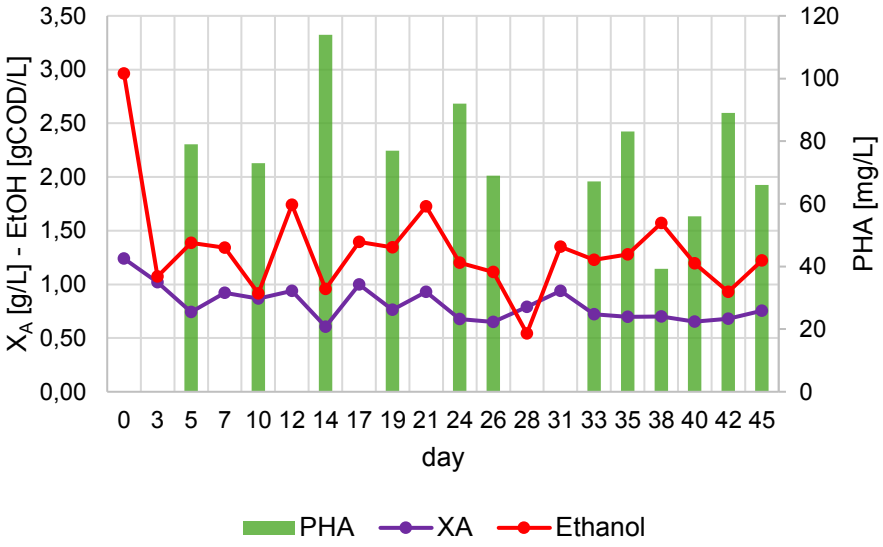

Figure 27: Active biomass, Ethanol and PHA trend - Run-2

As shown in Table 8, the PHA storage yield and the percentage of PHA contained in the bacteria have increased compared to run-1, due to the reduction in OLR and the consequences explained above. Since PHA yield production increased when the OLR was reduced, the third run maintained the same OLR and HRT, while introducing biomass recirculation to enhance biomass productivity.

Table 8: Active biomass concentration, %PHA, PHA and observed yields – Run-2

X_A	$Y_{PHA/S}^{feast}$	%PHA	Y_{OBS}^{SBR}
g/L	*$COD/COD_{removed}$*	*g/g VSS*	*$COD/COD_{removed}$*
0.79 ± 0.03	0.070 ± 0.004	9.7 ± 0.7	0.45 ± 0.02

4.2.3 Biomass nutritional profile characterisation

To investigate the potential of PPB biomass as a source of SCP, nutritional profile analyses were performed on the harvested biomass. The analyses were performed in duplicate, and the results are shown in Table 9. The protein content was slightly below the range reported in literature for PNSB species, which are known to produce a crude protein content ranging from 300 to 600 mg/gdry biomass (Rashid et al., 2024). The protein content was determined using Bradford method, which provides the protein content, and not the crude protein content. However, an optimized calibration was used and interferences were minimized, which allowed to compare the values with those in literature.

Table 9: Nutritional profile of lyophilized biomass – Run-2

	% in biomass	**Concentration in colture (mg/L)**	**mg/g$_{\text{dry weight}}$**
Carbohydrates	0.040 ± 0.002	0.41 ± 0.02	0.40 ± 0.02
Lipids	7.3 ± 0.3	75 ± 3	72 ± 3
Proteins	29 ± 1	298 ± 12	286 ± 11

4.3 Photobioreactor operation: Run-3

4.3.1 Feedstock characterisation

In the third condition, an OLR similar to that of the run-2 was tested, with an average value of 1.64 ± 0.07 $\frac{\text{gCOD}}{\text{L×d}}$. Additionally, an SRT of 4 days was applied to evaluate potential improvements in overall performances and nutritional profile resulting from the recirculated biomass. As for run-2, one liter of feedstock contained 150 mL of digestate, 80 mL of wine lees, and 770 mL of tap water. Moreover, ammonium chloride was added to reach an average concentration of 0.18 ± 0.04 g/L, in order to

compensate for the low ammonium content in the feedstock. Average values of the most relevant feedstock characteristics are summarized in Table 10.

Table 10: Feedstock characterisation - Run-3

pH	**TSS**	**VSS**	**COD_{SOL}**	**$N\text{-}NH_4^+$**	**EtOH**	**OAs (TOT)**	**$\frac{OAs+EtOH}{COD_{SOL}}$**
	g(TS)/L	*g(VS)/L*	*g(O_2)/L*	*g/L*	*gCOD/L*	*gCOD/L*	*COD/COD %*
6.8 ± 0.1	0.36 ± 0.07	0.32 ± 0.07	5.0 ± 0.2	0.18 ± 0.04	2.8 ± 0.1	0.50 ± 0.04	65 ± 3

The pH, TSS, VSS, COD_{SOL} and ethanol values increased compared to run-2. In particular, the TSS and VSS levels nearly doubled, although they remained low. The COD_{SOL} also increased by more than one unit, while the identified fraction of it decreased to 65%. These observed differences, compared to run-2, cannot be explained by the slight increase in the OLR alone. Instead, they are likely due to the intrinsic variability in the chemical composition of the real waste streams used as feedstock. Specifically, the composition of wine lees may have been altered by degradative processes that occurred during the extended storage period in the freezer, which lasted several months, as well as during the subsequent thawing. At the same time, the digestate may have undergone chemical composition changes as a result of the fluctuations in its feeding. As evidence of this, the chemical composition of the feedstock changed, as shown in Figure 28. While the ethanol percentage increased up to 85%, this run showed a different organic acids profile compared to runs 1 and 2, where acetic and propionic acids were present in comparable proportions, with a small contribution of butyric acid. In this run, acetic acid clearly dominated, with only a minimal amount of propionic acid, and no butyric acid was detected.

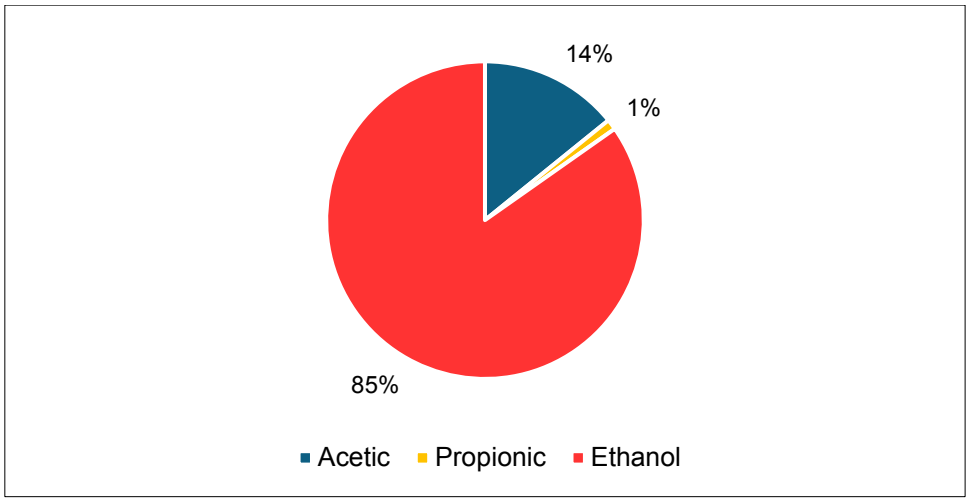

Figure 28: Organic acids profile in feedstock - Run-3

The temporal trend of OLR is shown in Figure 29. Similar to run-1, this run exhibits more pronounced fluctuations, particularly during the initial and final phases of the test, while a period of relative stability is observed in the middle. However, the most significant fluctuation occurred between day 9 (1.33 $\frac{gCOD}{L \times d}$) and day 16 (1.90 $\frac{gCOD}{L \times d}$), remaining within limited variational ranges. Once again, the OLR was effectively controlled throughout the entire experiment, even though the intrinsic chemical variations that characterize waste streams.

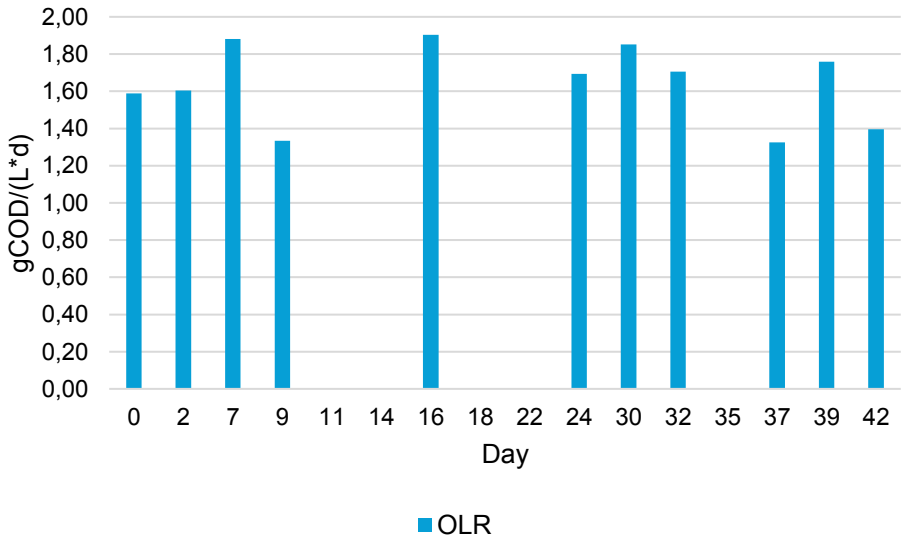

Figure 29: OLR trend – Run-3

4.3.2 Photobioreactor performances

In this run, biomass recirculation was introduced to achieve an SRT of 4 days. The VS/TS ratio of harvested biomass was 0.96, indicates that the vast majority of the solids reintroduced into the reactor, after centrifugation, consisted of organic matter, such as PPB biomass, with a very minimal contribution of inorganic fraction. As a result of the recirculation, the VSS concentration increased, showing an average value of 1. 7 ± 0.1 g/L. As shown in Figure 30, an upward VSS trend was observed in the first part of the test, likely due to the biomass adaptation. In the final two weeks, fluctuations were observed, coinciding with the oscillations in OLR values. The middle period was stable. The VSS/TSS ratio remained constant throughout the experiment, with an average value of 0.85 ± 0.01, confirming that PPB biomass constituted the majority of the solids in the reactor. Compared to run-1 and run-2, this ratio decreased, likely due to the small inorganic fraction reintroduced into the reactor in recirculation process. The recirculation increased the biomass productivity, resulting in an average value of 0.84 ± 0.05 gVSS/L*d.

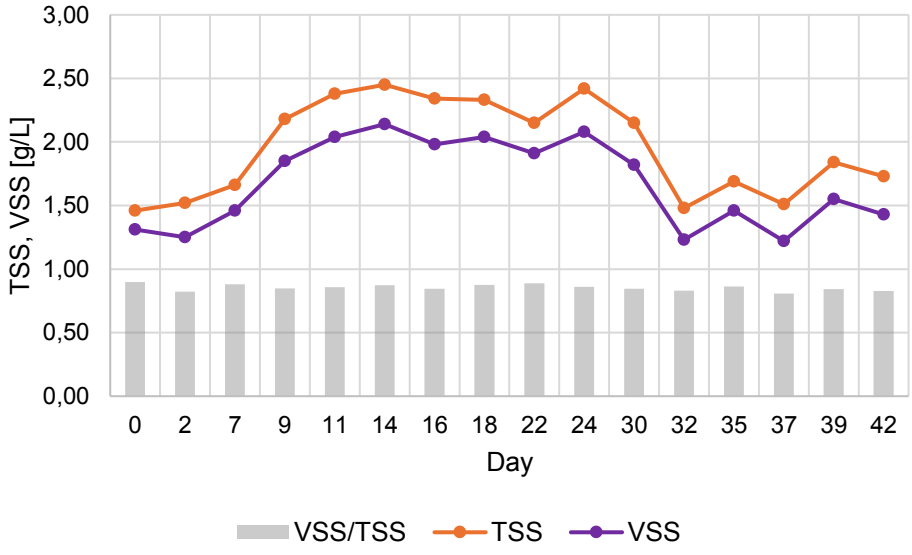

Figure 30: TSS, VSS and VSS/TSS trend - Run-3

The temporal trends of COD_{SOL}, ethanol and OAs_{TOT} both in the feedstock and the reactor effluent are shown in Figure 31. Compared to the other runs, the ethanol and COD_{SOL} trends in the effluent were characterized by fewer fluctuations, indicating a more stable substrate removal. The COD_{SOL} removal efficiency increased, reaching an average value of 57 ± 2%, with an average COD_{SOL} concentration in the reactor of 2.18

± 0.08 g/L, slightly higher than that observed in run-2 due to the higher COD_{SOL} concentration in the feedstock. Ethanol removal improved significantly compared to the other runs, reaching an average value of 70 ± 5%, which represented an increase of 16% compared to run-2. Among the OAs_{TOT} that were present in the reactor effluent, only acetic acid was detected, with an average concentration of 0.12 ± 0.01 g/L. The OAs_{TOT} removal was 76 ± 3%, lower than that in the other runs. This reduction could be attributed to possible degradation processes of COD_{SOL} and particulate matter caused by recirculation, which may have promoted fermentative processes. Overall, the increase in SRT enhanced the removal of ethanol and COD_{SOL}, while the removal of OAs_{TOT} remained high.

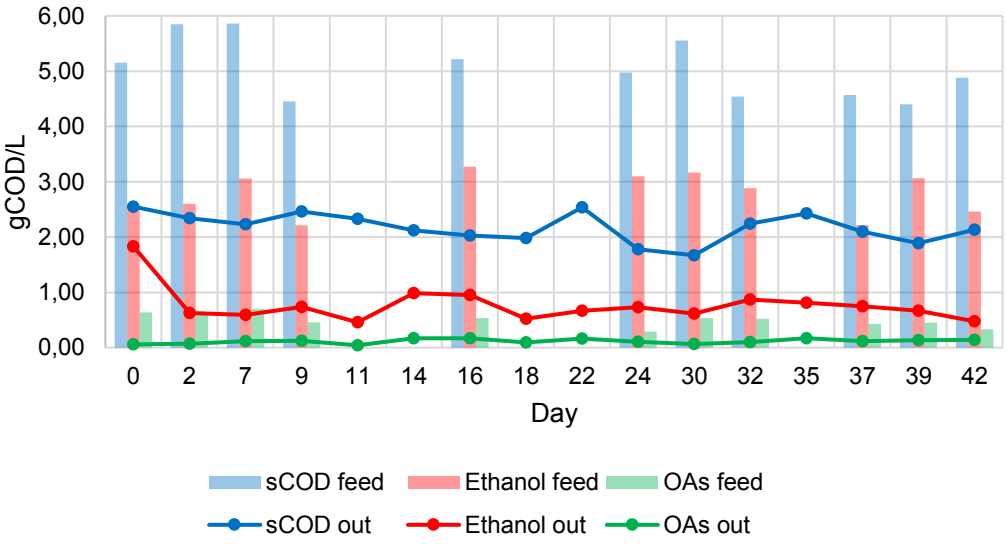

Figure 31: COD_{SOL}, Ethanol and OAsTOT trend – Run-3

Figure 32 illustrates the temporal trends of pH and ammonium. The pH remained relatively stable throughout the experiment (average value of 6.2 ± 0.2), except for two minor fluctuations observed in the middle. A decline in pH was noted, possibly due to acidogenic fermentative processes caused by the higher VS concentration in the mixed liquor. Even though fluctuations in the ammonium trend were detected, ammonium removal efficiency remained high, with an average value of 97 ± 0.7%, suggesting that, as in the other runs, almost all nitrogen was utilized for cellular growth.

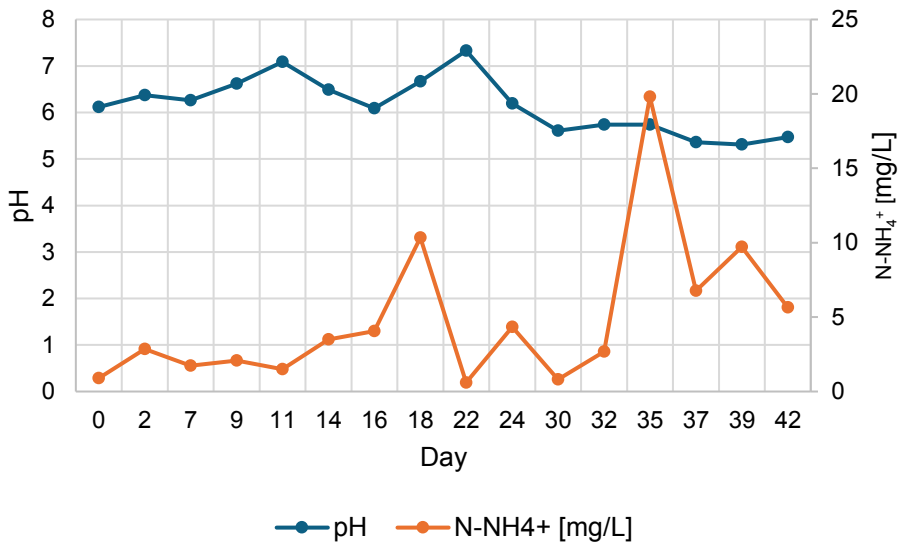

Figure 32: pH and N-NH_4^+ trend – Run-3

The temporal trend of biopolymers is shown in Figure 33. A stable biopolymers production was observed, with some fluctuations in the final days. Regarding the biopolymer composition, their percentage (wt%) is shown in Figure 34. The majority was represented by P3(HB), with an average value of 102 ± 4 mg/L, while the contribution of P3(HV) was modest, with an average value of 25 ± 2 mg/L.

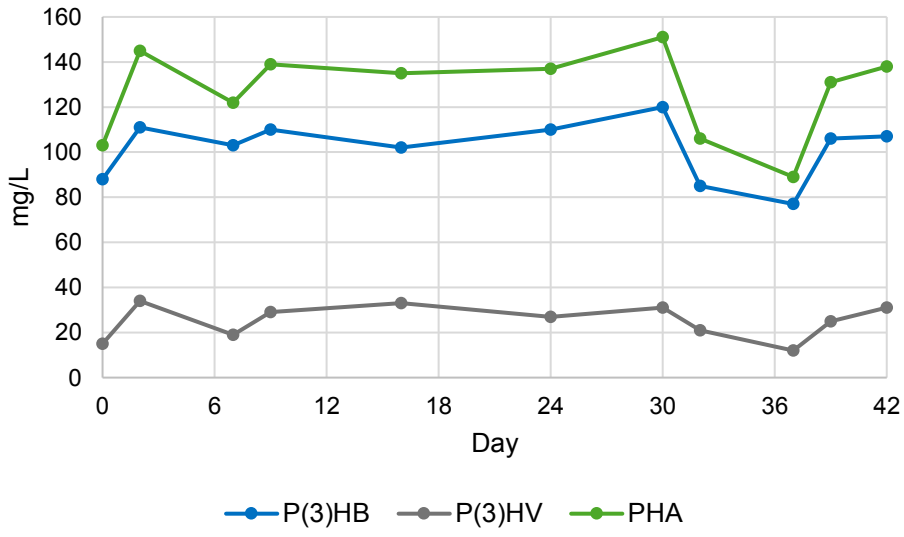

Figure 33: Biopolymers trend – Run-3

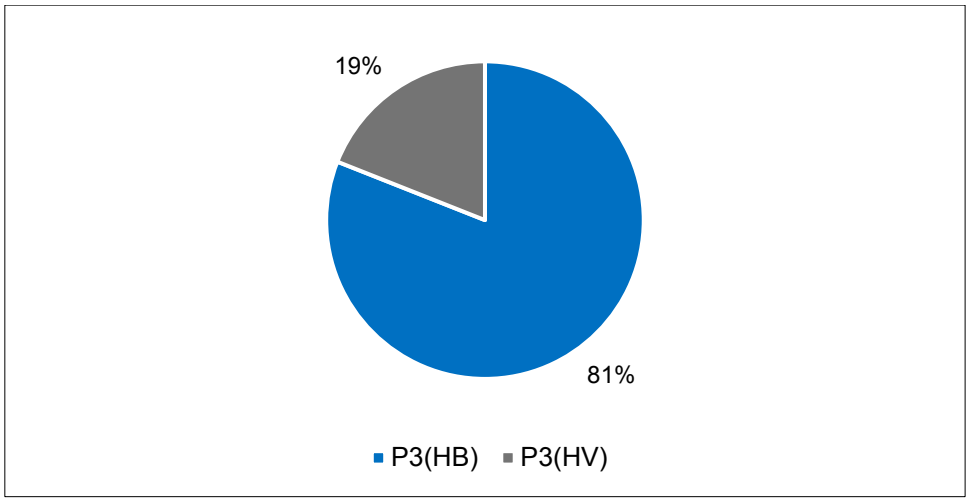

Figure 34: PHB and PHV percentage (wt%) – Run-3

Figure 35 compares the trends of active biomass (X_A), the PHA concentration, and the residual ethanol present in the reactor effluent. A similar trend was observed between biomass and PHA production, suggesting that biopolymer production was closely linked to biomass growth, characteristic of a permanent feast condition, as in this study (Montiel-Corona & Buitrón, 2022). However, some discrepancies emerged on specific days, indicating interesting metabolic dynamics. In particular, on day 30, a decrease in biomass, an increase in PHA concentration and a reduction of residual ethanol suggested that ethanol was preferentially used for PHA synthesis rather than biomass growth. Conversely, on day 32, ethanol concentration increased while both active biomass and PHA decreased. This dynamic may indicate a temporary interruption of metabolism, with ethanol accumulation not being immediately used for either cellular growth or biopolymer production. Subsequently, on day 39, a simultaneous increase in biomass and PHA was recorded, accompanied by a decrease in residual ethanol. This trend likely indicated efficient ethanol utilization as a substrate for both cell growth and PHA production. Finally, on day 42, a reduction in XA, a decrease in ethanol concentration and a slight increase in PHA content were observed. This scenario again suggested that residual ethanol was primarily used for biopolymer synthesis rather than biomass proliferation. Additionally, it is important to note that while the VSS concentration in the reactor increased due to the higher SRT, the ammonium chloride added to the feed remained the same as in run-1 and run-2. This may have led to nutrient limitation, which further enhanced PHA (Montiel-Corona & Buitrón, 2022). The observations above highlight the system's metabolic adaptability to changes in environmental and substrate conditions.

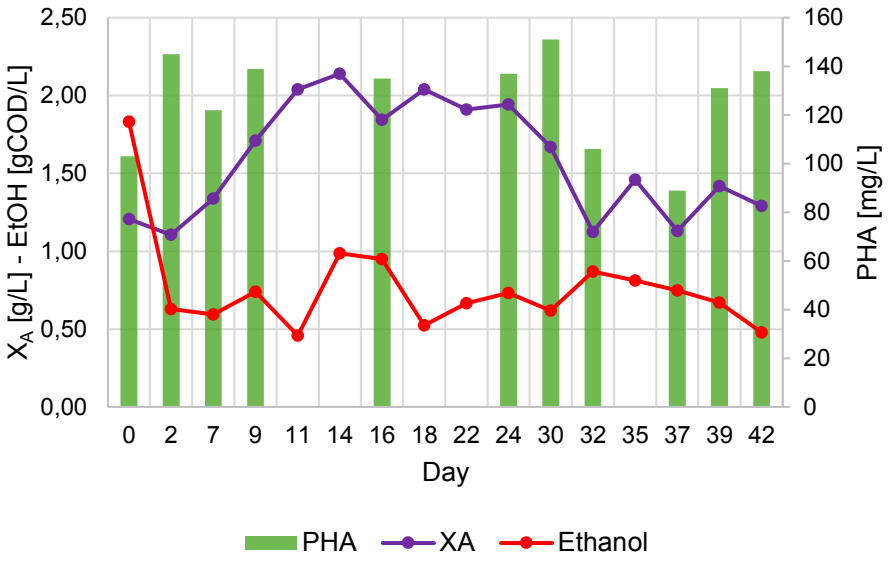

Figure 35: Active biomass, Ethanol and PHA trend - Run-3

As shown in Table 11, the increase in PHA concentration in the reactor effluent did not lead to a higher percentage of PHA within the biomass. This was likely due to the recirculation: the total amount of PHA increased, as a result of the higher VSS concentration in the reactor, but the PHA content in individual cells remained unchanged. However, both the storage PHA yield and the observed yield improved, due to the overall improved, likely due to the enhanced substrate assimilation and maybe due to the higher of acetate in the feedstock. As mentioned earlier, literature suggests that acetate is the most suitable carbon source (Rashid et al., 2024).

Table 11: Active biomass concentration, %PHA, PHA and observed yields – Run-3

X_A	$Y_{PHA/S}^{feast}$	%PHA	Y_{OBS}^{SBR}
g/L	*$COD/COD_{removed}$*	*g/g VSS*	*$COD/COD_{removed}$*
0.98 ± 0.06	0.09 ± 0.01	8.3 ± 0.6	0.55 ± 0.04

4.3.3 Biomass nutritional profile characterisation

Table 12 summarizes the average values of carbohydrates, lipids, and proteins in the lyophilized biomass. As in run-2, the analyses were performed in duplicate. The protein content increased, and was within the range reported in the literature for PNSB

biomass (300-600 mg/$g_{dry\ weight}$) (Rashid et al., 2024). A decrease in carbohydrate and lipid content was observed in comparison to the run-2, likely due to the increased in biopolymer production yield. In fact, the storage of PHA and lipids shares similar metabolic pathways, with acetyl-CoA as a common precursor (Argiz et al., 2022). However, under nitrogen limitation conditions, PHA accumulation is preferential over lipids (Argiz et al., 2022). This could explain the reduction in lipid content during this run.

Table 12: Nutritional profile of lyophilized biomass – Run-3

	% in biomass	**Concentration in colture (mg/L)**	**mg/$g_{dry\ weight}$**
Carbohydrates	0.022 ± 0.001	0.365 ± 0.009	0.223 ± 0.005
Lipids	5.5 ± 0.2	91 ± 2	55 ± 2
Proteins	45 ± 4	744 ± 69	454 ± 42

4.4 Comparison between SBR runs

A comparison of the various parameters detected in the reactor effluent in all three experimental runs is presented in Table 13. Since VSS/TSS ratio was high in every run, the TSS average value is not shown in the table. In run-1, characterized by the highest pH and OLR, it was observed a relatively high VSS and PHA values. However, the intracellular PHA percentage was lower than in the other two runs. This can be attributed to the continuous feast condition driven by the high OLR. It is possible that PPB, living in an ethanol-rich environment, had firstly prioritized cellular growth over PHA accumulation, and then storage PHA as stress mechanism when ethanol concentration exceeded a certain threshold. In fact, this run had the lowest PHA production yield and the lowest SBR observed yield. In terms of OAS_{TOT} removal, this run exhibited the highest value. Conversely, run-2 operated under a lower OLR and a more acid pH. In these conditions, VSS level decreased, but the intracellular PHA percentage increased, despite a lower PHA concentration compared to run-1. This phenomenon can be attributed to the limited substrate availability caused by the

reduced OLR, stimulating PPB to synthetize PHA as energy storage, rather than prioritize cell growth. This can explains the lower biomass productivity compared to run-1. Furthermore, run-2 exhibited the lowest removal efficiencies, except for ammonium removal, which was higher than in run-1. In the third run, biomass recirculation was introduced, an OLR similar to run-2 was used and a more acid pH in the reactor effluent was detected. This configuration led to a general improvement in system performances. COD_{SOL} and ethanol removal efficiencies increased, likely due to enhanced substrate utilization driven by the higher VSS value in the reactor. In particular, ethanol removal increased up to 70%, a significant improvement compared to the previous runs. Additionally, the SBR observed yield increased up to 0.55. Although the intracellular PHA percentage was lower than in run-2, the higher biomass concentration in the reactor resulted in a higher PHA concentration. Moreover, the PHA production yield nearly doubled compared to run-1, suggesting that, unlike the other runs where ethanol and COD_{SOL} removal was lower, in this run the substrate was more extensively consumed for both cell growth and PHA production. This enhancement was accompanied by an increase in the SBR observed yield and biomass productivity, suggesting a positive correlation between biomass growth and PHA production. For all the three runs, the most produced biopolymer was P3(HB), with the highest P3(HV) percentage in run-1. Finally, the SBR observed yield for all three runs was consistent and within the range reported in the literature for waste stream substrates (0.2–0.7 $COD/gCOD_{removed}$) (Rashid et al., 2024). It worthy remembering that the PHA storage yield was underestimated for all three runs, since PHA concentration was measured 4 hours after the feeding phase of a cycle, while the $COD_{removed}$ was calculated 12 hours after that. Nevertheless, all three runs exhibited an interesting PHA% content within cells, consistently above 8%. As previously mentioned, high PHA accumulation is not necessary in feed applications, such as in aquaculture, where beneficial effects are achieved with inclusion rate ranging from 0.2 to 5 wt% (Santhosh and Umesh, 2021). Therefore, the PHA levels observed in all three runs are suitable for this purpose. A quantitative analysis of the correlations between the measured parameters should have been conducted, in order to confirm and expand the above hypothesis, and provide further insights into the metabolic strategies adopted by the biomass. An important consideration for all three runs concerns the TSS and VSS values in the feedstock. Although low, they are not negligible, and stricter filtration should have been implemented to prevent interference with the VSS value in the reactor. In terms of the

nutritional profile of lyophilized biomass from runs 2 and 3, run 3 once again showed better results. In fact, its protein content was higher than that of run 2, aligning with the range reported in the literature for PNSB species (Rashid et al., 2024).

Table 13: Comparison of the various parameters detected in the reactor effluent in all three experimental runs

	pH	OLR	VSS	COD_{SOL}	$N\text{-}NH_4^+$	EtOH	OAs_{TOT}	$N\text{-}NH_4^+$ removv.	COD_{SOL} removv.
		$\frac{gCOD}{L \times d}$	$\frac{gVS}{L}$	$\frac{gCOD}{L}$	$\frac{mg}{L}$	$\frac{gCOD}{L}$	$\frac{gCOD}{L}$	%	%
Run 1	7.7 ± 0.2	2.74 ± 0.09	1.03 ± 0.06	3.4 ± 0.3	1.9 ± 0.8	1.6 ± 0.1	0.04 ± 0.01	94 ± 3	50 ± 5
Run 2	6.1 ± 0.1	1.61 ± 0.04	0.84 ± 0.03	2.21 ± 0.09	1.1 ± 0.2	1.24 ± 0.07	0.09 ± 0.01	96 ± 1	43 ± 4
Run 3	6.2 ± 0.2	1.64 ± 0.07	1.7 ± 0.1	2.18 ± 0.08	5 ± 2	0.8 ± 0.1	0.12 ± 0.01	97 ± 1	57 ± 2

	EtOH removv	OAs_{TOT} removv	PHB	PHV	PHA	%PHA	$Y_{PHA/S}^{feast}$	Y_{OBS}^{SBR}	PPB Productivity
	%	%	$\frac{mg}{L}$	$\frac{mg}{L}$	$\frac{mg}{L}$	$\frac{gPHA}{gVSS}$	$\frac{COD}{COD}$	$\frac{COD}{COD}$	$\frac{gVSS}{L \times d}$
Run 1	59 ± 4	96 ± 3	73 ± 4	30 ± 2	102 ± 6	8.7 ± 0.5	0.05 ± 0.01	0.33 ± 0.02	0.54 ± 0.03
Run 2	54 ± 2	83 ± 3	63 ± 4	12 ± 3	75 ± 5	9.7 ± 0.7	0.07 ± 0.01	0.45 ± 0.02	0.42 ± 0.01
Run 3	70 ± 5	76 ± 3	102 ± 4	25 ± 2	127 ± 6	8.3 ± 0.4	0.09 ± 0.01	0.55 ± 0.04	0.84 ± 0.05

5. Conclusions

The aim of this thesis was to investigate part of a multi-step bioprocess focused on SCP production through the cultivation of PPB using not fermented wine lees (WL) as feedstock. The main goal was to produce PHA-rich biomass while valorizing a by-product of the wine industry, supporting the principles of circular economy and improving the sustainability of the bioactive SCP production chain for aquaculture. The research explored the influence of OLR, HRT and SRT on PPB growth in a lab-scale 2-L SBR. In order to reduce SCP production costs, this study employed a non-sterile mixed microbial culture (MMC) of PPB and unfermented WL, avoiding dark fermentation step to simplifying operational phases. The results highlighted that run-1, characterized by the highest OLR, promoted active bacterial growth despite of the high level of ethanol in the media. High OLR, however, limited PHA accumulation and yield. Conversely, the reduced OLR in run-2 led to a higher percentage of PHA within cells, presumably as a bacterial response and adaption to readily biodegradable substrate (VFA) scarcity. Biomass recirculation adopted in run-3 played a crucial role in stabilizing the system and enhancing substrate conversion into biopolymers, maximizing both PHA production and biomass yield. Moreover, run-3 achieved the best biomass growth and PHA concentration balance, optimizing metabolic efficiency, stabilizing the system, and increasing biopolymer production. Overall, the differences between run-1 and run-2 highlight how substrate availability affected the balance between cell growth and energy reserve accumulation as PHA. A relatively high OLR in run-1 stimulated biomass growth, while PHA production was more associated with ethanol-induced stress. Limited VFA availability in run-2 led bacteria to prioritized PHA production rather than cell growth. The biomass recirculation in run-3 optimized overall metabolism, leading to better system performances and higher PHA production yield. Regarding the use of PPB as a value-added protein ingredient in feed applications (aquaculture, among others) the protein content in the third run reached approximately 454 mg/$g_{dry\ biomass}$. This value is lower than the value reported by Alloul et al., (2021) in their study conducted on shrimps (approximately 737 mg/$g_{dry\ biomass}$). However, as noted by Delamare-Debouteville et al. (2019), PPB biomass does not need to completely replace traditional feed, and even when included in moderate amounts, it can provide beneficial effects. Additionally, the PPB biomass in all three runs contained more PHA to that the minimum required to observe beneficial effects in aquaculture

(Santhosh and Umesh, 2021). Therefore, the PHA levels observed in all three runs are suitable for this application.

Overall, this study demonstrated that unfermented WL can be effectively valorized as a feedstock for PHA-rich SCP production using a mixed microbial culture of PPB, simultaneously reducing overall production costs. For future research, it would be necessary to analyse the aminoacidic profile and pigments' content in the biomass, to obtain a more comprehensive understanding of the nutritional profile of PPB for aquaculture feed applications. Additionally, an analysis of other nutrients, such as phosphorus, could reveal whether PHA production is associated with other nutrients availability or scarcity. Investigating the bacterial genera and species involved would also be useful to optimize their growth conditions, and conducting experiments under light stress could help to determine if biomass and PHA production can be enhanced. Moreover, since hydrogen and PHA production share similar metabolic pathways and often compete for the reducing power within the cell (Capson-Tojo et al., 2020), it would be appropriate to examine whether hydrogen production occurs.

Nevertheless, this study offers valuable insights, as there are few studies in the literature that explore the use of an ethanol-rich real substrate, such as wine lees, to cultivate a mixed microbial culture (MMC) of PPB in a non-sterile environment.

References

Ahmad, B., Yadav, V., Yadav, A., Rahman, M. U., Yuan, W. Z., Li, Z., & Wang, X. (2020). Integrated biorefinery approach to valorize winery waste: A review from waste to energy perspectives. *Science of the Total Environment*, *719*. https://doi.org/10.1016/j.scitotenv.2020.137315

Allegue, L. D., Puyol, D., & Melero, J. A. (2020). Novel approach for the treatment of the organic fraction of municipal solid waste: Coupling thermal hydrolysis with anaerobic digestion and photo-fermentation. *Science of the Total Environment*, *714*. https://doi.org/10.1016/j.scitotenv.2020.136845

Alloul, A., Wille, M., Lucenti, P., Bossier, P., Van Stappen, G., & Vlaeminck, S. E. (2021). Purple bacteria as added-value protein ingredient in shrimp feed: Penaeus vannamei growth performance, and tolerance against Vibrio and ammonia stress. *Aquaculture*, *530*. https://doi.org/10.1016/j.aquaculture.2020.735788

Anderson, A. J., & Dawes, E. A. (1990). Occurrence, Metabolism, Metabolic Role, and Industrial Uses of Bacterial Polyhydroxyalkanoates. In *MICROBIOLOGICAL REVIEWS* (Vol. 54, Issue 4). https://journals.asm.org/journal/mr

Argiz, L., Correa-Galeote, D., Val del Río, Á., Mosquera-Corral, A., & González-Cabaleiro, R. (2022). Valorization of lipid-rich wastewaters: A theoretical analysis to tackle the competition between polyhydroxyalkanoate and triacylglyceride-storing populations. *Science of the Total Environment*, *807*. https://doi.org/10.1016/j.scitotenv.2021.150761

Basak, N., Jana, A. K., Das, D., & Saikia, D. (2014). Photofermentative molecular biohydrogen production by purple-non-sulfur (PNS) bacteria in various modes: The present progress and future perspective. In *International Journal of Hydrogen Energy* (Vol. 39, Issue 13, pp. 6853–6871). Elsevier Ltd. https://doi.org/10.1016/j.ijhydene.2014.02.093

Bilal, M., Asgher, M., Iqbal, H. M. N., Hu, H., & Zhang, X. (2017). Biotransformation of lignocellulosic materials into value-added products—A review. In *International Journal of Biological Macromolecules* (Vol. 98, pp. 447–458). Elsevier B.V. https://doi.org/10.1016/j.ijbiomac.2017.01.133

Bleakley, S., & Hayes, M. (2017). Algal proteins: Extraction, application, and challenges concerning production. *Foods*, *6*(5), 1–34. https://doi.org/10.3390/foods6050033

Bolzonella, D., Papa, M., Da Ros, C., Anga Muthukumar, L., & Rosso, D. (2019). Winery wastewater treatment: a critical overview of advanced biological processes. In *Critical Reviews in Biotechnology* (Vol. 39, Issue 4, pp. 489–507). Taylor and Francis Ltd. https://doi.org/10.1080/07388551.2019.1573799

Bustos, G., Moldes, A. B., Cruz, J. M., & Domínguez, J. M. (2004). Formulation of Low-Cost Fermentative Media for Lactic Acid Production with Lactobacillus rhamnosus Using Vinification Lees as Nutrients. *Journal of Agricultural and Food Chemistry*, *52*(4), 801–808. https://doi.org/10.1021/jf030429k

Candebat, C. L., Booth, M. A., & Pirozzi, I. (2021). The sulfur amino acid requirements of juvenile Yellowtail Kingfish (Seriola lalandi). *Aquaculture*, *534*. https://doi.org/10.1016/j.aquaculture.2020.736234

Capson-Tojo, G., Batstone, D. J., Grassino, M., Vlaeminck, S. E., Puyol, D., Verstraete, W., Kleerebezem, R., Oehmen, A., Ghimire, A., Pikaar, I., Lema, J. M., & Hülsen, T. (2020). Purple phototrophic bacteria for resource recovery: Challenges and opportunities. In *Biotechnology Advances* (Vol. 43). Elsevier Inc. https://doi.org/10.1016/j.biotechadv.2020.107567

Chen, Y. T., Wu, S. C., & Lee, C. M. (2012). Relationship between cell growth, hydrogen production and poly-β-hydroxybutyrate (PHB) accumulation by Rhodopseudomonas palustris WP3-5. *International Journal of Hydrogen Energy*, *37*(18), 13887–13894. https://doi.org/10.1016/j.ijhydene.2012.06.024

Chumpol, S., Kantachote, D., Nitoda, T., & Kanzaki, H. (2018). Administration of purple nonsulfur bacteria as single cell protein by mixing with shrimp feed to enhance growth, immune response and survival in white shrimp (Litopenaeus vannamei) cultivation. *Aquaculture*, *489*, 85–95. https://doi.org/10.1016/j.aquaculture.2018.02.009

Da Ros, C., Cavinato, C., Pavan, P., & Bolzonella, D. (2017). Mesophilic and thermophilic anaerobic co-digestion of winery wastewater sludge and wine lees: An integrated approach for sustainable wine production. *Journal of Environmental Management*, *203*, 745–752. https://doi.org/10.1016/j.jenvman.2016.03.029

De Iseppi, A., Lomolino, G., Marangon, M., & Curioni, A. (2020). Current and future strategies for wine yeast lees valorization. In *Food Research International* (Vol. 137). Elsevier Ltd. https://doi.org/10.1016/j.foodres.2020.109352

De Schryver, P., Sinha, A. K., Kunwar, P. S., Baruah, K., Verstraete, W., Boon, N., De Boeck, G., & Bossier, P. (2010). Poly-β-hydroxybutyrate (PHB) increases growth performance and intestinal bacterial range-weighted richness in juvenile European sea bass, Dicentrarchus labrax. *Applied Microbiology and Biotechnology*, *86*(5), 1535–1541. https://doi.org/10.1007/s00253-009-2414-9

Defoirdt, T., Halet, D., Vervaeren, H., Boon, N., Van De Wiele, T., Sorgeloos, P., Bossier, P., & Verstraete, W. (2007). The bacterial storage compound poly-β-hydroxybutyrate protects Artemia franciscana from pathogenic Vibrio campbellii. *Environmental Microbiology*, *9*(2), 445–452. https://doi.org/10.1111/j.1462-2920.2006.01161.x

Delamare-Deboutteville, J., Batstone, D. J., Kawasaki, M., Stegman, S., Salini, M., Tabrett, S., Smullen, R., Barnes, A. C., & Hülsen, T. (2019). Mixed culture purple phototrophic bacteria is an effective fishmeal replacement in aquaculture. *Water Research X*, *4*. https://doi.org/10.1016/j.wroa.2019.100031

Devesa-Rey, R., Vecino, X., Varela-Alende, J. L., Barral, M. T., Cruz, J. M., & Moldes, A. B. (2011). Valorization of winery waste vs. the costs of not recycling. *Waste Management*, *31*(11), 2327–2335. https://doi.org/10.1016/j.wasman.2011.06.001

Dimou, C., Kopsahelis, N., Papadaki, A., Papanikolaou, S., Kookos, I. K., Mandala, I., & Koutinas, A. A. (2015). Wine lees valorization: Biorefinery development including production of a generic fermentation feedstock employed for poly(3-hydroxybutyrate) synthesis. *Food Research International*, *73*, 81–87. https://doi.org/10.1016/j.foodres.2015.02.020

Eklund, E. (1983). The antimicrobial effect of dissociated and undissociated sorbic acid at different pH levels. In *Journal of Applied Bacteriology* (Vol. 54).

Fradinho, J. C., Reis, M. A. M., & Oehmen, A. (2016). Beyond feast and famine: Selecting a PHA accumulating photosynthetic mixed culture in a permanent feast regime. *Water Research*, *105*, 421–428. https://doi.org/10.1016/j.watres.2016.09.022

Gamboa-Delgado, J., & Márquez-Reyes, J. M. (2018). Potential of microbial-derived nutrients for aquaculture development. In *Reviews in Aquaculture* (Vol. 10, Issue 1, pp. 224–246). Wiley-Blackwell. https://doi.org/10.1111/raq.12157

Geyer, T., & Helms, V. (2006). Reconstruction of a kinetic model of the chromatophore vesicles from Rhodobacter sphaeroides. *Biophysical Journal*, *91*(3), 927–937. https://doi.org/10.1529/biophysj.105.067561

Gottardo, M., Bolzonella, D., Adele Tuci, G., Valentino, F., Majone, M., Pavan, P., & Battista, F. (2022). Producing volatile fatty acids and polyhydroxyalkanoates from foods by-products and waste: A review. In *Bioresource Technology* (Vol. 361). Elsevier Ltd. https://doi.org/10.1016/j.biortech.2022.127716

Hartigan, N., Tharia, H. A., Sweeney, F., Lawless, A. M., & Papiz, M. Z. (2002). The 7.5-Å electron density and spectroscopic properties of a novel low-light B800 LH2 from Rhodopseudomonas palustris. *Biophysical Journal*, *82*(2), 963–977. https://doi.org/10.1016/S0006-3495(02)75456-8

Hülsen, T., Barnes, A. C., Batstone, D. J., & Capson-Tojo, G. (2022). Creating value from purple phototrophic bacteria via single-cell protein production. In *Current Opinion in Biotechnology* (Vol. 76). Elsevier Ltd. https://doi.org/10.1016/j.copbio.2022.102726

Jones, S. W., Karpol, A., Friedman, S., Maru, B. T., & Tracy, B. P. (2020). Recent advances in single cell protein use as a feed ingredient in aquaculture. In

Current Opinion in Biotechnology (Vol. 61, pp. 189–197). Elsevier Ltd. https://doi.org/10.1016/j.copbio.2019.12.026

Kim, J. K., Lee, B.-K., Kim, S.-H., & Moon, J.-H. (1999). Characterization of denitrifying photosynthetic bacteria isolated from photosynthetic sludge. In *Aquacultural Engineering* (Vol. 19).

Kucek, L. A., Xu, J., Nguyen, M., & Angenent, L. T. (2016). Waste conversion into n-caprylate and n-caproate: Resource recovery from wine lees using anaerobic reactor microbiomes and in-line extraction. *Frontiers in Microbiology*, *7*(NOV). https://doi.org/10.3389/fmicb.2016.01892

Laranja, J. L. Q., & Bossier, P. (2020). Poly-Beta-Hydroxybutyrate (PHB) and Infection Reduction in Farmed Aquatic Animals. In *Health Consequences of Microbial Interactions with Hydrocarbons, Oils, and Lipids* (pp. 457–482). Springer International Publishing. https://doi.org/10.1007/978-3-030-15147-8_35

Laranja, J. L. Q., De Schryver, P., Ludevese-Pascual, G. L., Amar, E. C., Aerts, M., Vandamme, P., & Bossier, P. (2018). High amorphous poly-beta-hydroxybutyrate (PHB) content in a probiotic Bacillus strain displays better protective effects in Vibrio-challenged gnotobiotic Artemia. *Aquaculture*, *487*, 15–21. https://doi.org/10.1016/j.aquaculture.2018.01.005

Lu, H., Zhang, G., Zheng, Z., Meng, F., Du, T., & He, S. (2019). Bio-conversion of photosynthetic bacteria from non-toxic wastewater to realize wastewater treatment and bioresource recovery: A review. In *Bioresource Technology* (Vol. 278, pp. 383–399). Elsevier Ltd. https://doi.org/10.1016/j.biortech.2019.01.070

Matassa, S., Batstone, D. J., Hülsen, T., Schnoor, J., & Verstraete, W. (2015). Can direct conversion of used nitrogen to new feed and protein help feed the world? *Environmental Science and Technology*, *49*(9), 5247–5254. https://doi.org/10.1021/es505432w

Matassa, S., Boon, N., Pikaar, I., & Verstraete, W. (2016). Microbial protein: future sustainable food supply route with low environmental footprint. *Microbial Biotechnology*, *9*(5), 568–575. https://doi.org/10.1111/1751-7915.12369

Melnicki, M. R., Eroglu, E., & Melis, A. (2009). Changes in hydrogen production and polymer accumulation upon sulfur-deprivation in purple photosynthetic bacteria. *International Journal of Hydrogen Energy*, *34*(15), 6157–6170. https://doi.org/10.1016/j.ijhydene.2009.05.115

Miles, R. D., & Chapman, F. A. (n.d.). *The Benefits of Fish Meal in Aquaculture Diets 1*. http://edis.ifas.ufl.edu.

Moldes, A. B., Vázquez, M., Domínguez, J. M., Díaz-Fierros, F., & Barral, M. T. (2008). Negative effect of discharging vinification lees on soils. *Bioresource Technology*, *99*(13), 5991–5996. https://doi.org/10.1016/j.biortech.2007.10.004

Molina-Alcaide, E., Moumen, A., & Martín-García, A. I. (2008). By-products from viticulture and the wine industry: Potential as sources of nutrients for ruminants. *Journal of the Science of Food and Agriculture*, *88*(4), 597–604. https://doi.org/10.1002/jsfa.3123

Montiel-Corona, V., & Buitrón, G. (2022). Polyhydroxybutyrate production in one-stage by purple phototrophic bacteria: Influence of alkaline pH, ethanol, and C/N ratios. *Biochemical Engineering Journal*, *189*. https://doi.org/10.1016/j.bej.2022.108715

Muhammadi, Shabina, Afzal, M., & Hameed, S. (2015). Bacterial polyhydroxyalkanoates-eco-friendly next generation plastic: Production, biocompatibility, biodegradation, physical properties and applications. *Green Chemistry Letters and Reviews*, *8*(3–4), 56–77. https://doi.org/10.1080/17518253.2015.1109715

Navarro, P., Sarasa, J., Sierra, D., Esteban, S., & Ovelleiro, J. L. (n.d.). *Degradation of wine industry wastewaters by photocatalytic advanced oxidation*.

Neil Hunter, C., Daldal, F., Thurnauer, M. C., & Thomas Beatty, J. (n.d.). *The Purple Phototrophic Bacteria (Advances in Photosynthesis and Respiration, 28)*. www.springer.com/series/5599

EEC Regulation No.337/79, *Official Journal of the European Communities*.

Oliveira, M., & Duarte, E. (2016). Integrated approach to winery waste: waste generation and data consolidation. *Frontiers of Environmental Science and Engineering*, *10*(1), 168–176. https://doi.org/10.1007/s11783-014-0693-6

Paradelo, R., Moldes, A. B., & Barral, M. T. (2013). Evolution of organic matter during the mesophilic composting of lignocellulosic winery wastes. *Journal of Environmental Management*, *116*, 18–26. https://doi.org/10.1016/j.jenvman.2012.12.001

Pérez-Bibbins, B., Torrado-Agrasar, A., Pérez-Rodríguez, N., Aguilar-Uscanga, M. G., & Domínguez, J. M. (2015). Evaluation of the liquid, solid and total fractions of beer, cider and wine lees as economic nutrient for xylitol production. *Journal of Chemical Technology and Biotechnology*, *90*(6), 1027–1039. https://doi.org/10.1002/jctb.4405

Pérez-Bibbins, B., Torrado-Agrasar, A., Salgado, J. M., Oliveira, R. P. de S., & Domínguez, J. M. (2015). Potential of lees from wine, beer and cider manufacturing as a source of economic nutrients: An overview. *Waste Management*, *40*, 72–81. https://doi.org/10.1016/j.wasman.2015.03.009

Pesante, G., Zuliani, A., Cannone, E., Greco, F., Tesoriero, C., Vettori, A., & Frison, N. (2022). Biological conversion of agricultural residues into microbial proteins

for aquaculture using PHA-producing mixed microbial cultures. *Journal of Cleaner Production*, *378*. https://doi.org/10.1016/j.jclepro.2022.134554

Ragauskas, A. J., Williams, C. K., Davison, B. H., Britovsek, G., Cairney, J., Eckert, C. A., Frederick, W. J., Hallett, J. P., Leak, D. J., Liotta, C. L., Mielenz, J. R., Murphy, R., Templer, R., & Tschaplinski, T. (n.d.). *The Path Forward for Biofuels and Biomaterials*. https://www.science.org

Rashid, N., Onwusogh, U., & Mackey, H. R. (2024). Exploring the metabolic features of purple non-sulfur bacteria for waste carbon utilization and single-cell protein synthesis. In *Biomass Conversion and Biorefinery* (Vol. 14, Issue 12, pp. 12653–12672). Springer Science and Business Media Deutschland GmbH. https://doi.org/10.1007/s13399-022-03273-8

Ravindra, P. (2000). Value-added food: Single cell protein. In *Biotechnology Advances* (Vol. 18).

Rockenbach, I. I., Gonzaga, L. V., Rizelio, V. M., Gonçalves, A. E. de S. S., Genovese, M. I., & Fett, R. (2011). Phenolic compounds and antioxidant activity of seed and skin extracts of red grape (Vitis vinifera and Vitis labrusca) pomace from Brazilian winemaking. *Food Research International*, *44*(4), 897–901. https://doi.org/10.1016/j.foodres.2011.01.049

Ruberto, G., Renda, A., Daquino, C., Amico, V., Spatafora, C., Tringali, C., & Tommasi, N. De. (2007). Polyphenol constituents and antioxidant activity of grape pomace extracts from five Sicilian red grape cultivars. *Food Chemistry*, *100*(1), 203–210. https://doi.org/10.1016/j.foodchem.2005.09.041

Sakarika, M., Spanoghe, J., Sui, Y., Wambacq, E., Grunert, O., Haesaert, G., Spiller, M., & Vlaeminck, S. E. (2020). Purple non-sulphur bacteria and plant production: benefits for fertilization, stress resistance and the environment. In *Microbial Biotechnology* (Vol. 13, Issue 5, pp. 1336–1365). John Wiley and Sons Ltd. https://doi.org/10.1111/1751-7915.13474

Sandmann, G. (2021). Diversity and origin of carotenoid biosynthesis: its history of coevolution towards plant photosynthesis. In *New Phytologist* (Vol. 232, Issue 2, pp. 479–493). John Wiley and Sons Inc. https://doi.org/10.1111/nph.17655

Santhosh, A. S., & Umesh, M. (2021). A Strategic Review on Use of Polyhydroxyalkanoates as an Immunostimulant in Aquaculture. *Applied Food Biotechnology*, *8*(1), 1–18. https://doi.org/10.22037/afb.v8i1.31255

Shipman, R. H., Fan, L. T., & Kaol, I. C. (n.d.). *Single-Cell Protein Production by Photosynthetic Bacteria*.

STATE OF THE WORLD VINE AND WINE SECTOR IN 2022. (n.d.).

The State of World Fisheries and Aquaculture 2024. (2024). In *The State of World Fisheries and Aquaculture 2024*. FAO. https://doi.org/10.4060/cd0683en

Vasiliadou, I. A., Melero, J. A., Molina, R., Puyol, D., & Martinez, F. (2020). Optimization of H2 production through minimization of CO2 emissions by mixed cultures of purple phototrophic bacteria in aqueous samples. *Water (Switzerland)*, *12*(7). https://doi.org/10.3390/w12072015

Wade, N. M., Cheers, S., Bourne, N., Irvin, S., Blyth, D., & Glencross, B. D. (2017). Dietary astaxanthin levels affect colour, growth, carotenoid digestibility and the accumulation of specific carotenoid esters in the Giant Tiger Shrimp, Penaeus monodon. *Aquaculture Research*, *48*(2), 395–406. https://doi.org/10.1111/are.12888

Wang, X., Jiang, X. R., Wu, F., Ma, Y., Che, X., Chen, X., Liu, P., Zhang, W., Ma, X., & Chen, G. Q. (2019). Microbial Poly-3-Hydroxybutyrate (PHB) as a Feed Additive for Fishes and Piglets. *Biotechnology Journal*, *14*(12). https://doi.org/10.1002/biot.201900132

Yu, J., Plackett, D., & Chen, L. X. L. (2005). Kinetics and mechanism of the monomeric products from abiotic hydrolysis of poly[(R)-3-hydroxybutyrate] under acidic and alkaline conditions. *Polymer Degradation and Stability*, *89*(2), 289–299. https://doi.org/10.1016/j.polymdegradstab.2004.12.026

Yue, H., Zhao, C., Li, K., & Yang, S. (2015). Selective repression of light harvesting complex 2 formation in Rhodobacter azotoformans by light under semiaerobic conditions. *Journal of Basic Microbiology*, *55*(11), 1319–1325. https://doi.org/10.1002/jobm.201500178